Precision Mechatronics Laboratory

Leaf-spring suspension of a vertical inertial sensor for active seismic isolation

M. Zeoli, A. Amorosi, L. Amez-Droz, C. Collette

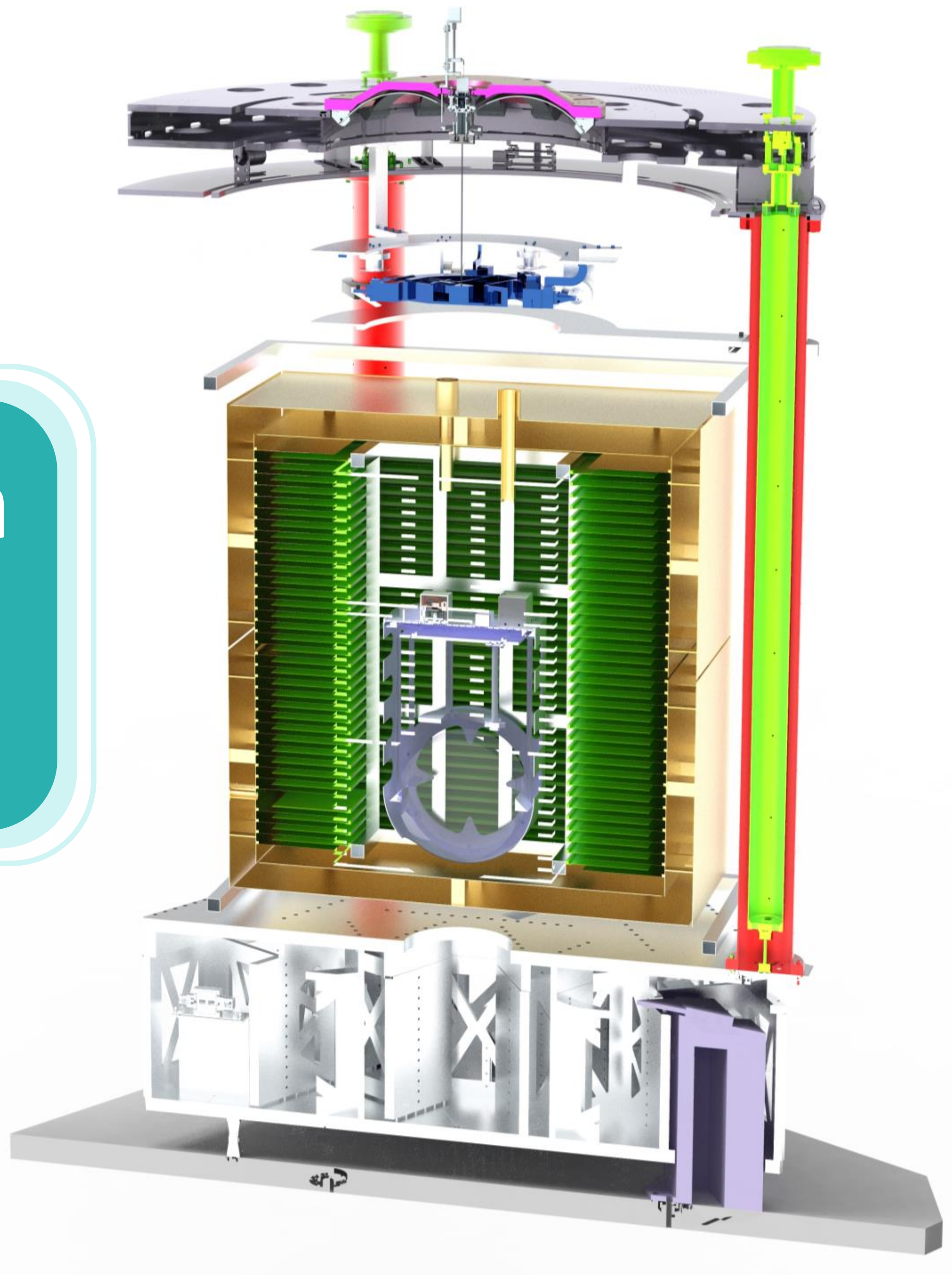

E-TEST Einstein Telescope EMR Site & Technology

Active seismic isolation

High frequency isolation

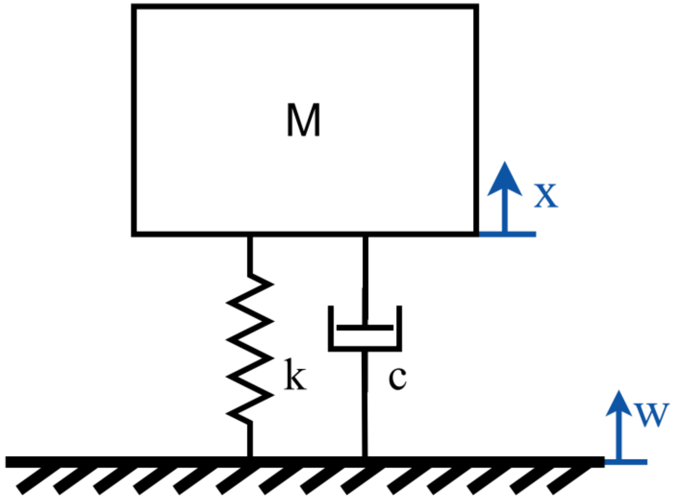

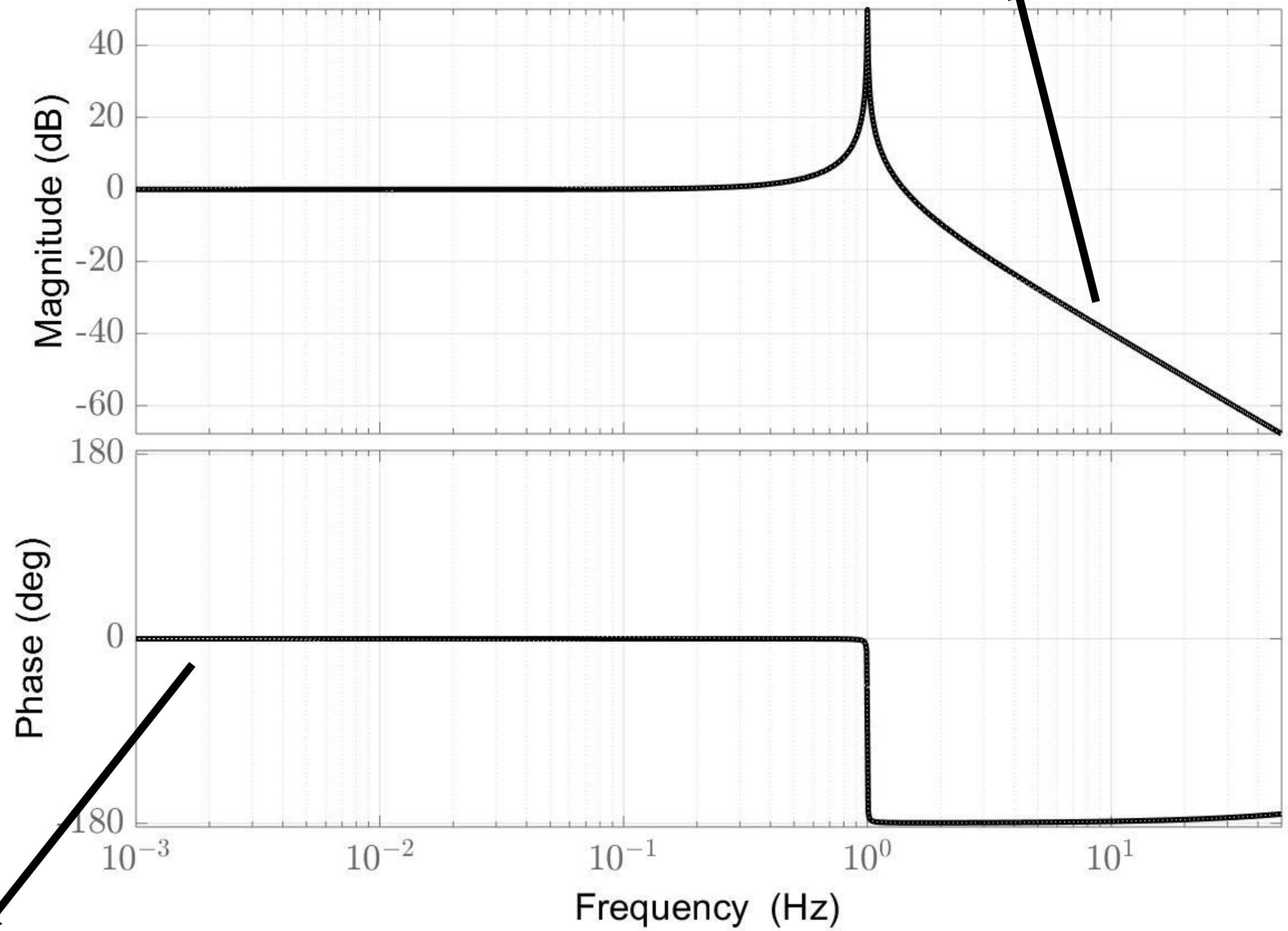

The equipment follows rigidly the ground

Transmissibility: $T_{wx} = \frac{X}{W}$

Active seismic isolation

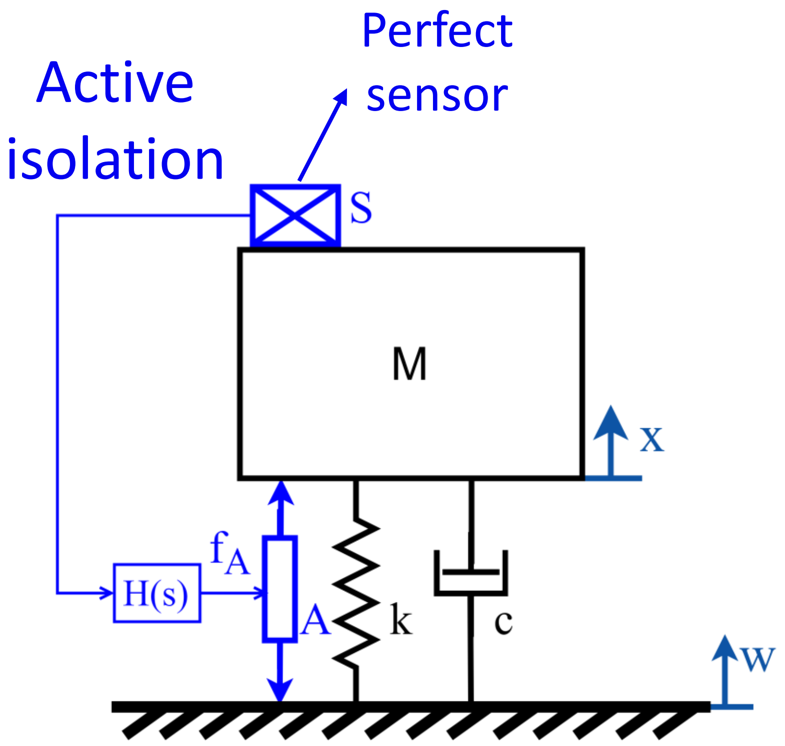

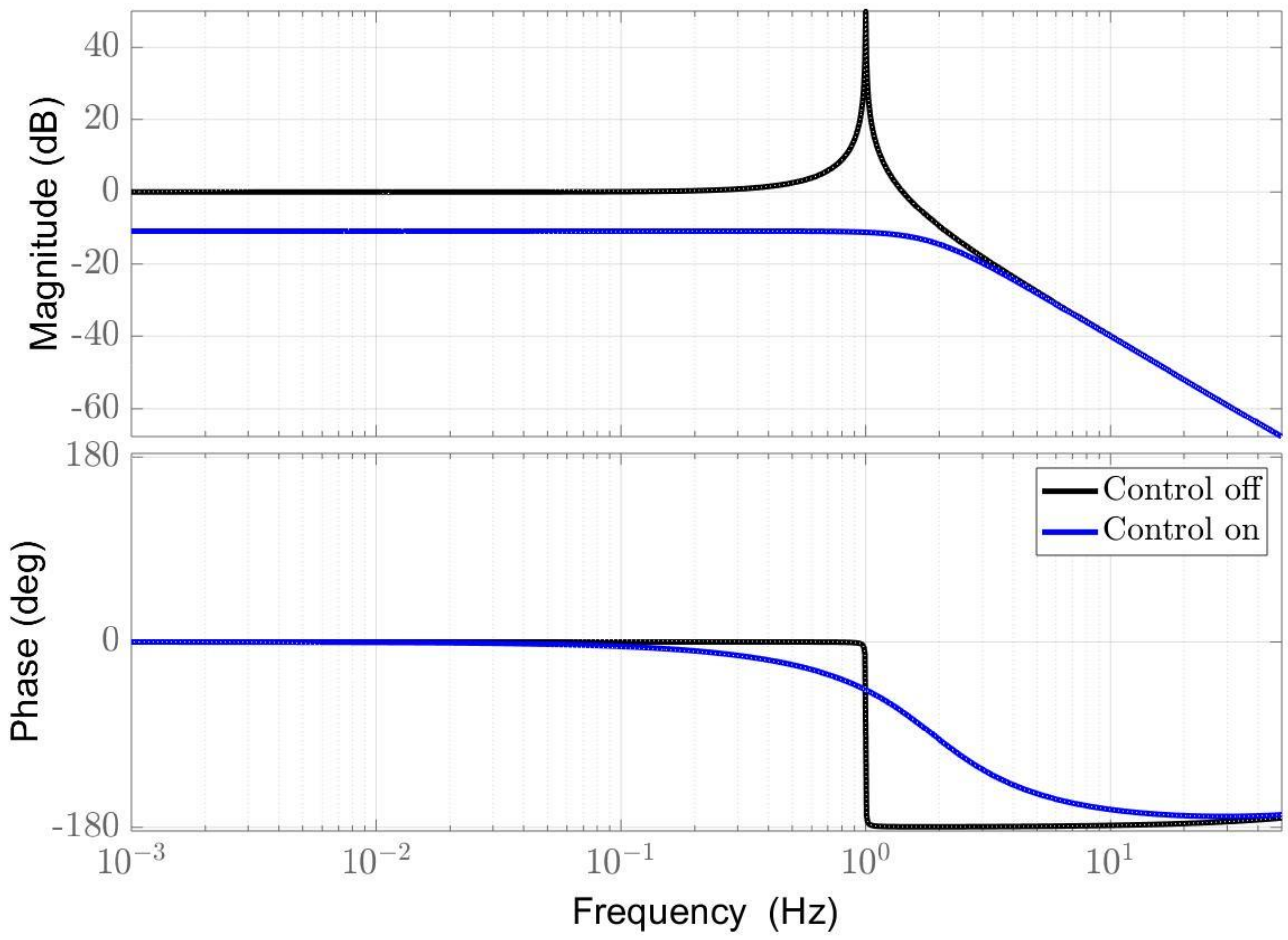

Transmissibility: $T_{wx} = \frac{X}{W}$

Active seismic isolation

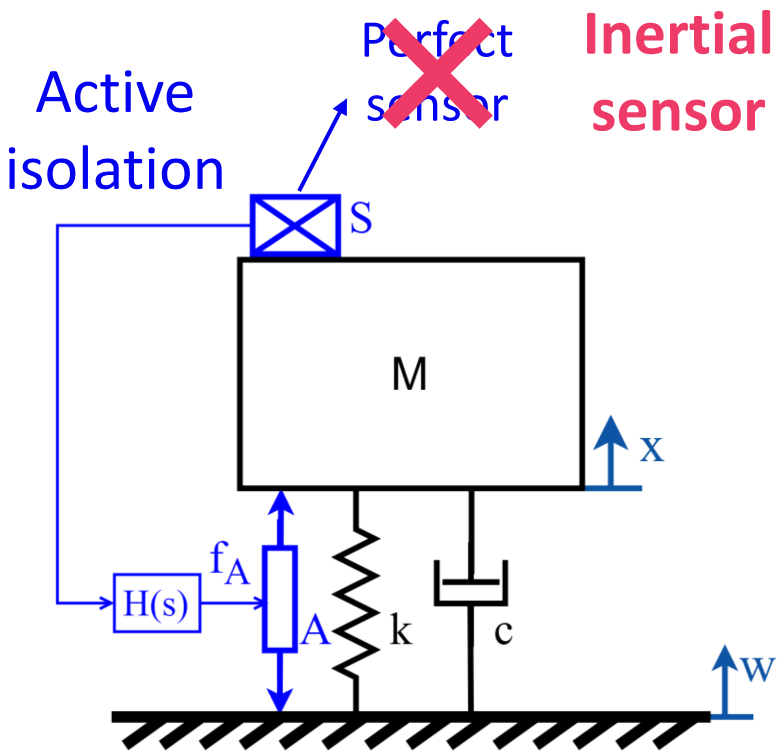

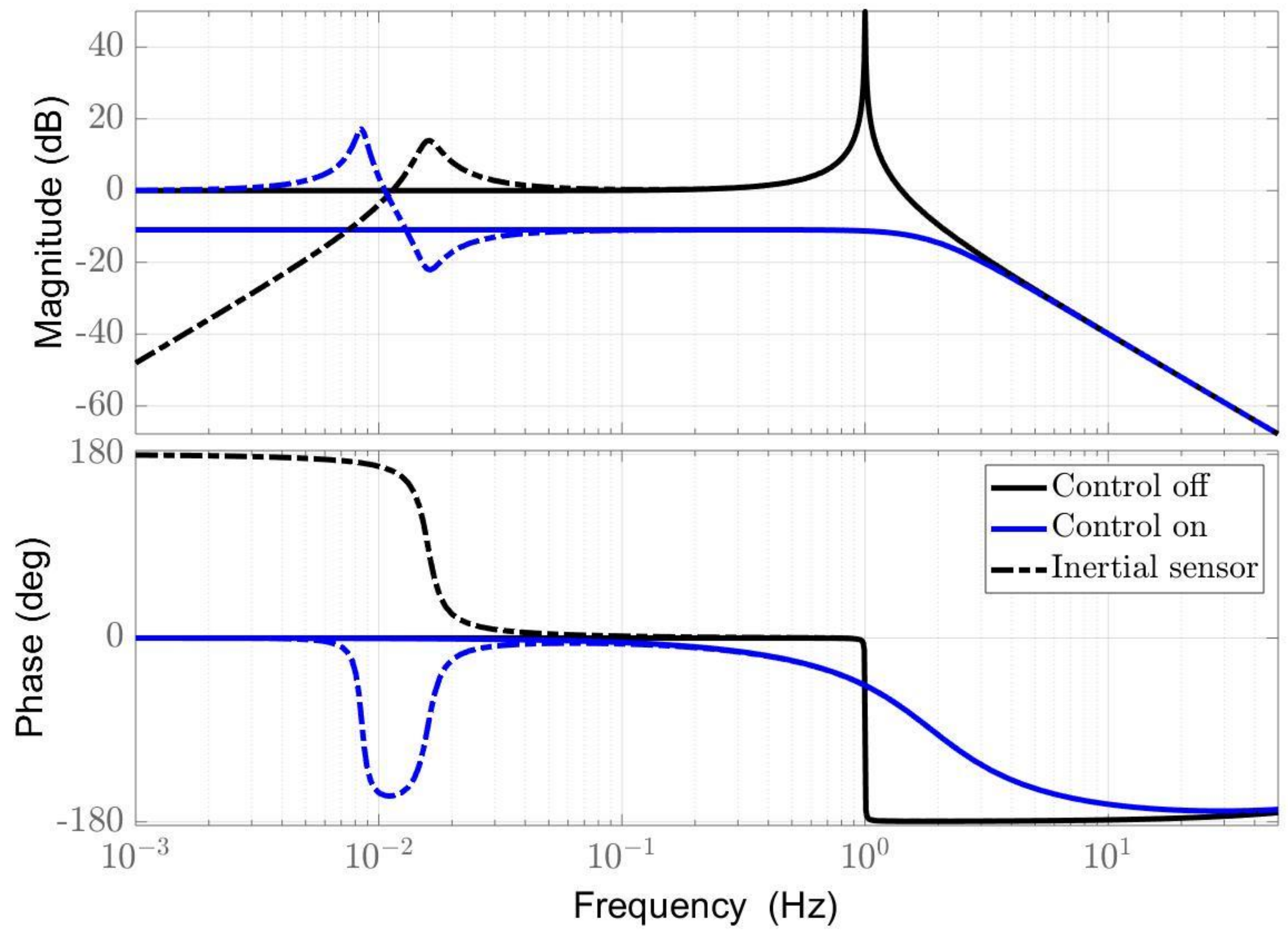

Transmissibility: $T_{wx} = \frac{X}{W}$

Active seismic isolation

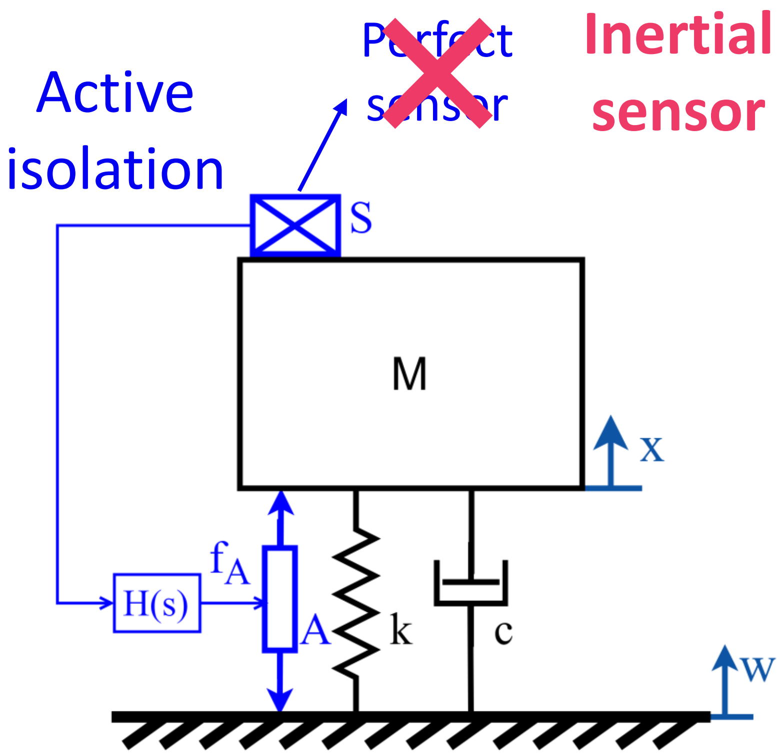

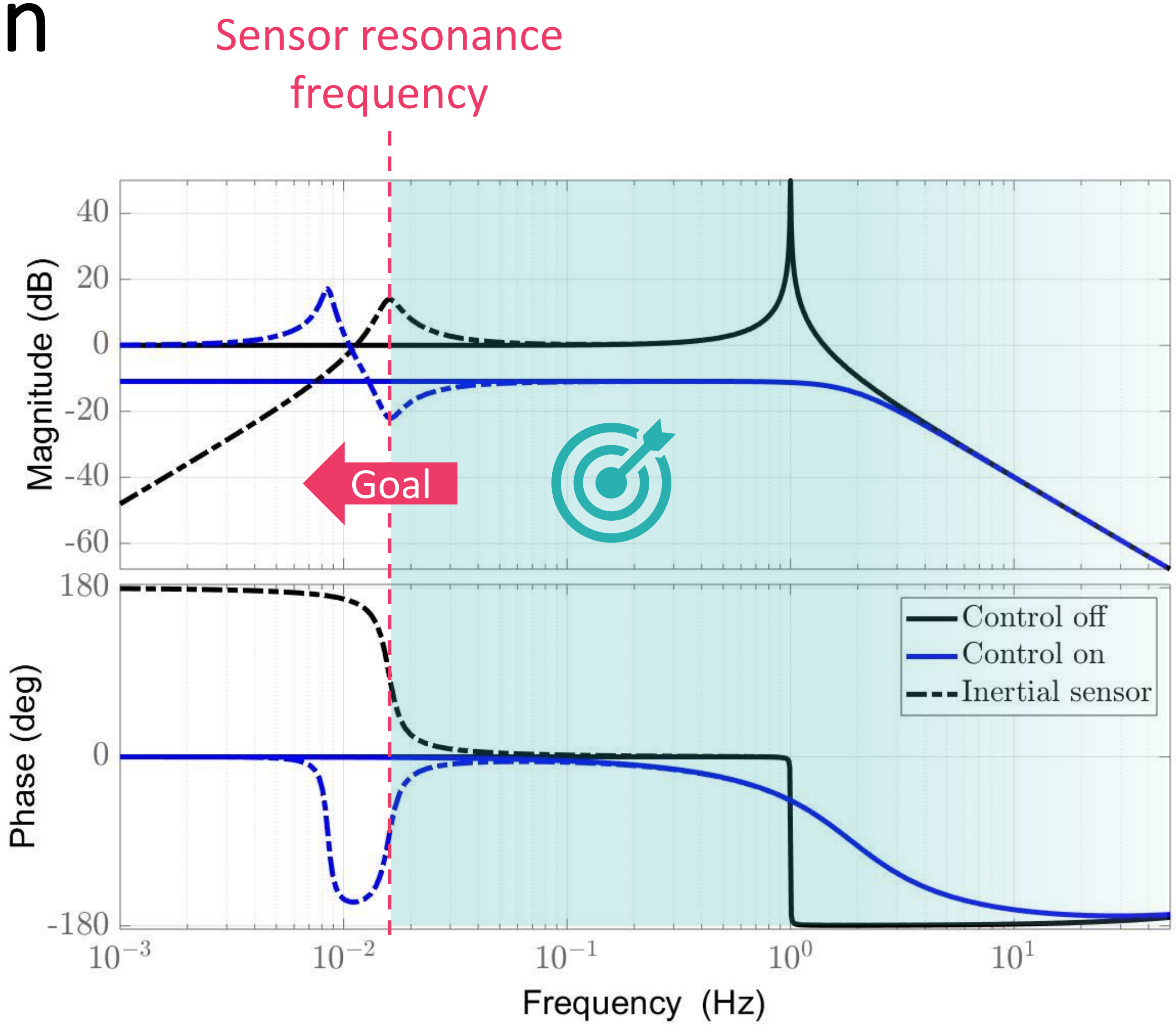

Transmissibility: $T_{wx} = \frac{X}{W}$

µVINS & studied parameters

$$f_0 = \frac{1}{2\pi}\sqrt{\frac{k}{m}}$$

Quasi-zero stiffness mechanism

Rotation

$$f_0^{(1)} = \frac{1}{2\pi}\sqrt{\frac{k_{\mathrm{LF}} r_s^2 + \kappa_{\mathrm{flex}}}{I}}$$

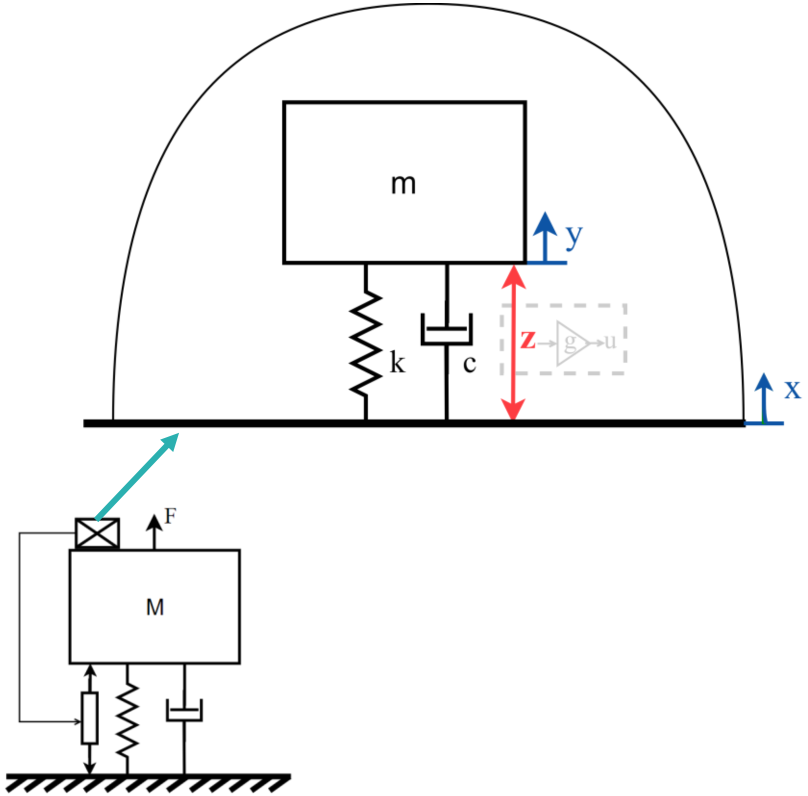

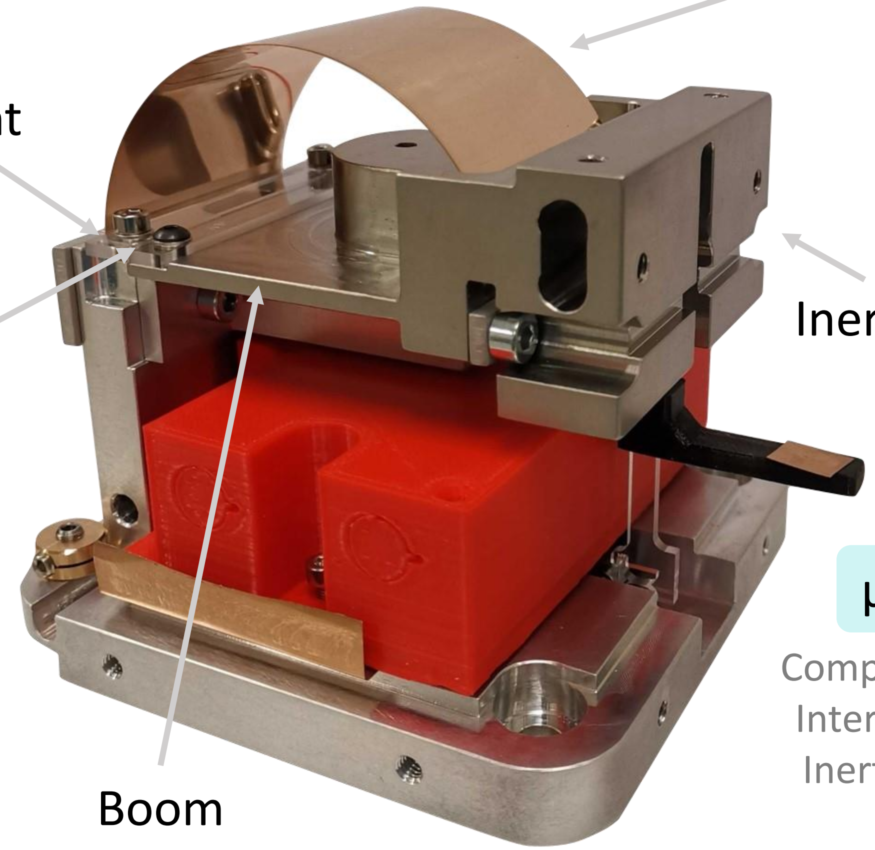

µVINS

Compact Vertical Interferometric Inertial Sensor

µVINS & studied parameters

$$f_0 = \frac{1}{2\pi}\sqrt{\frac{k}{m}}$$

Quasi-zero stiffness mechanism

Rotation

$$f_0^{(1)} = \frac{1}{2\pi}\sqrt{\frac{k_{\mathrm{LF}} r_s^2 + \kappa_{\mathrm{flex}}}{I}}$$

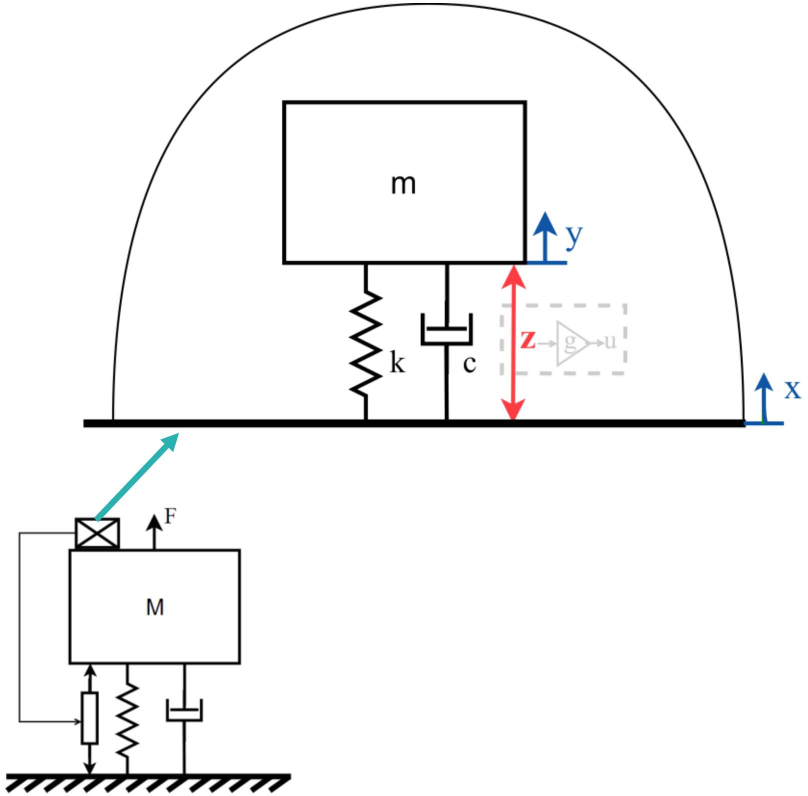

External clamping point

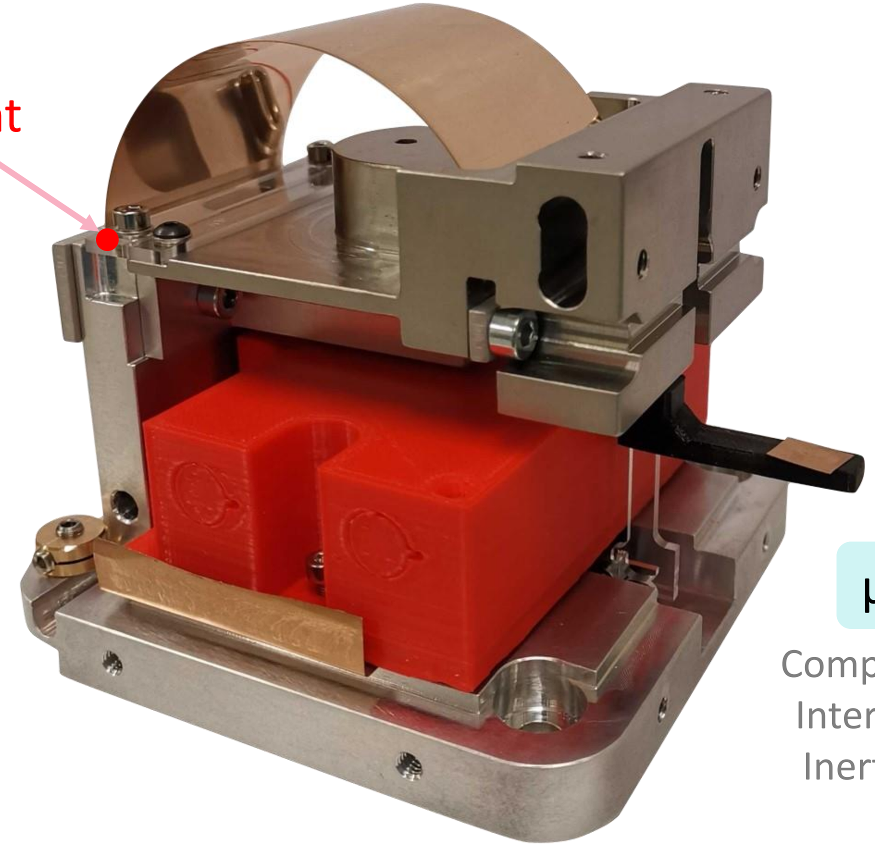

µVINS

Compact Vertical Interferometric Inertial Sensor

µVINS & studied parameters

$$f_0 = \frac{1}{2\pi}\sqrt{\frac{k}{m}}$$

Quasi-zero stiffness mechanism

Rotation

$$f_0^{(1)} = \frac{1}{2\pi}\sqrt{\frac{k_{\mathrm{LF}} r_s^2 + \kappa_{\mathrm{flex}}}{I}}$$

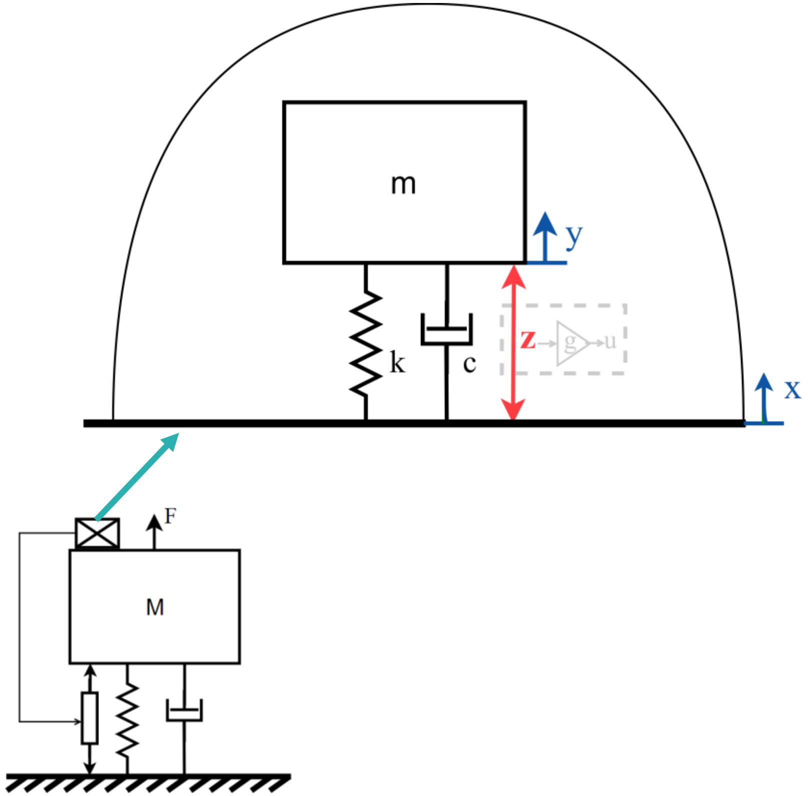

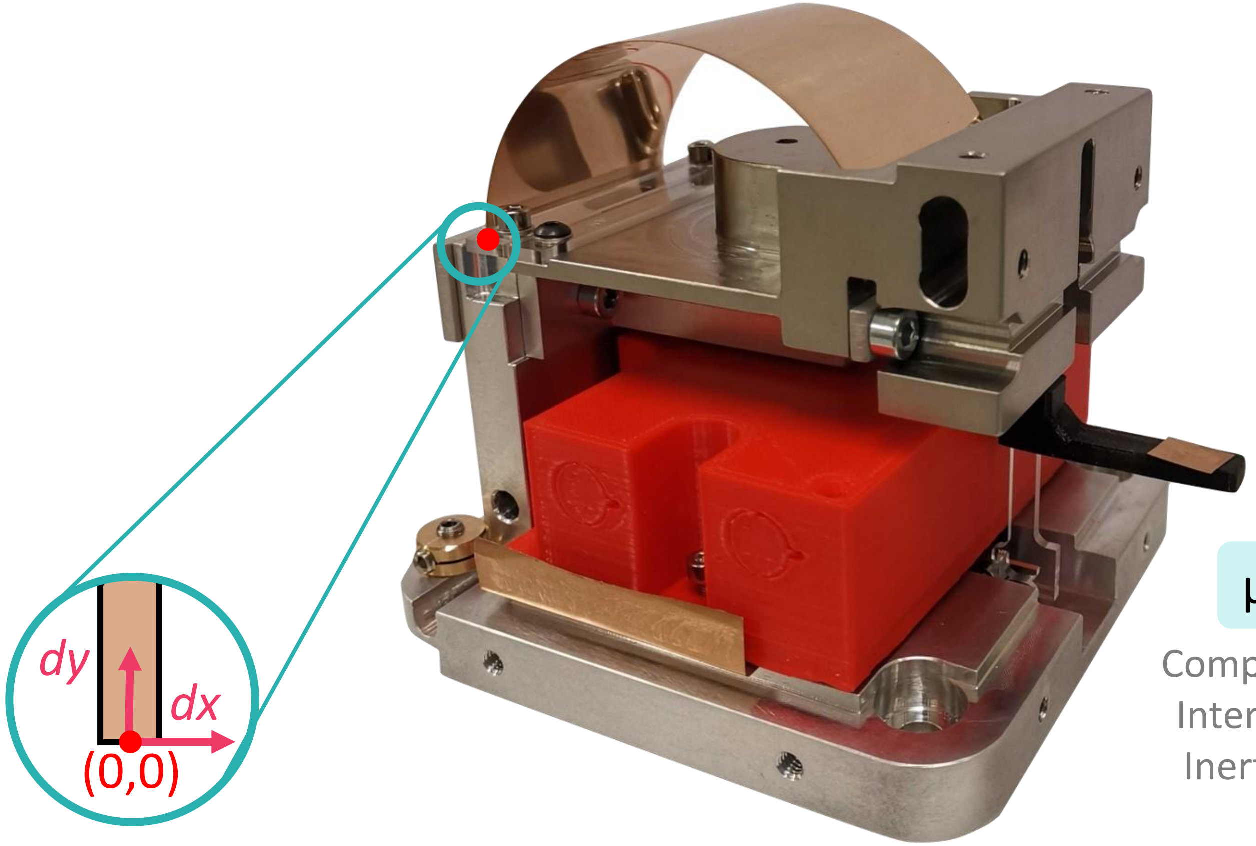

µVINS

Compact Vertical Interferometric Inertial Sensor

µVINS & studied parameters

$$f_0 = \frac{1}{2\pi}\sqrt{\frac{k}{m}}$$

Quasi-zero stiffness mechanism

Rotation

$$f_0^{(1)} = \frac{1}{2\pi}\sqrt{\frac{k_{\mathrm{LF}} r_s^2 + \kappa_{\mathrm{flex}}}{I}}$$

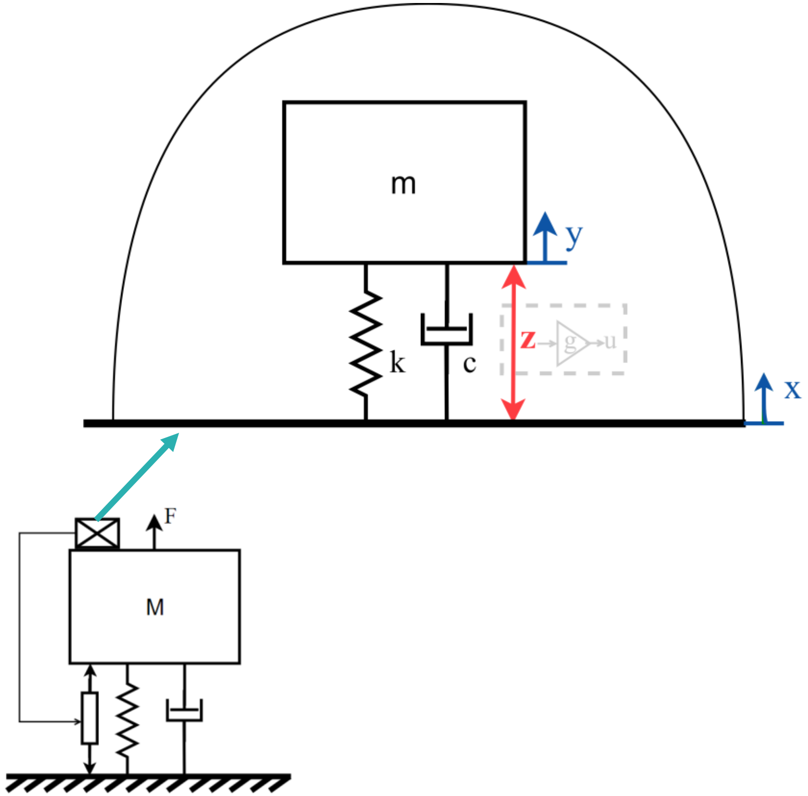

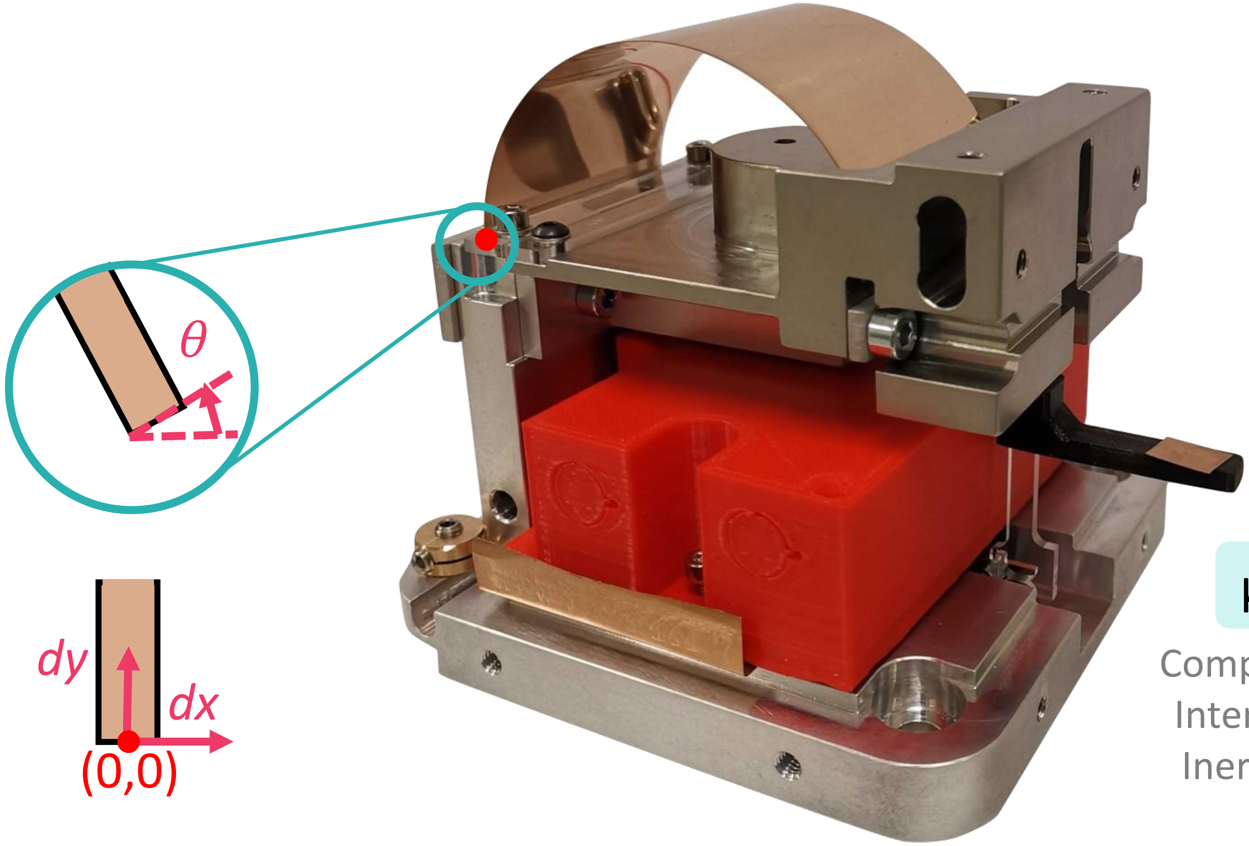

µVINS

Compact Vertical Interferometric Inertial Sensor

µVINS & studied parameters

$$f_0 = \frac{1}{2\pi}\sqrt{\frac{k}{m}}$$

Quasi-zero stiffness mechanism

Rotation

$$f_0^{(1)} = \frac{1}{2\pi}\sqrt{\frac{k_{\mathrm{LF}} r_s^2 + \kappa_{\mathrm{flex}}}{I}}$$

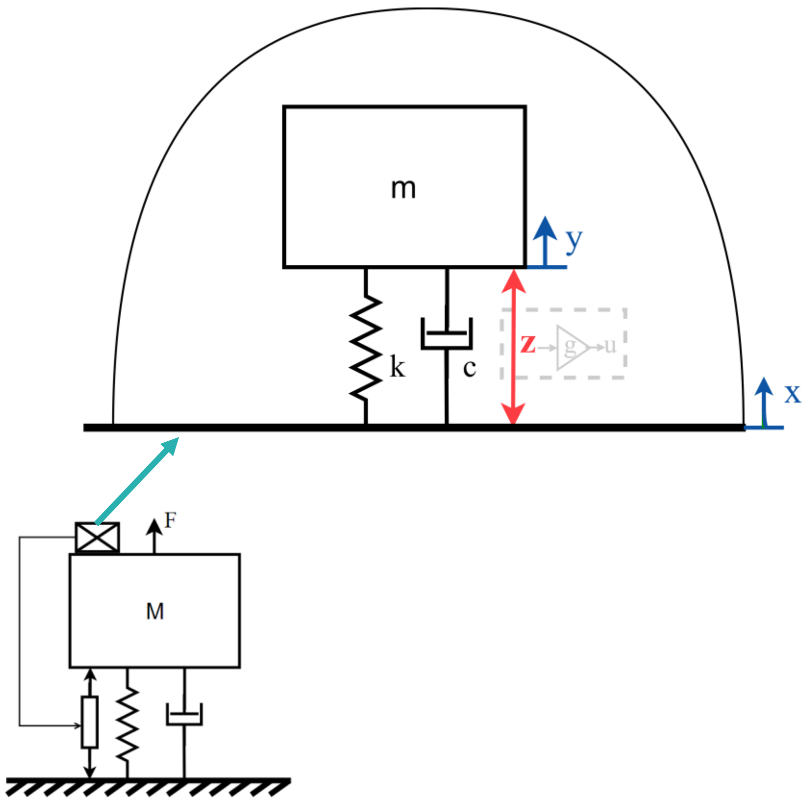

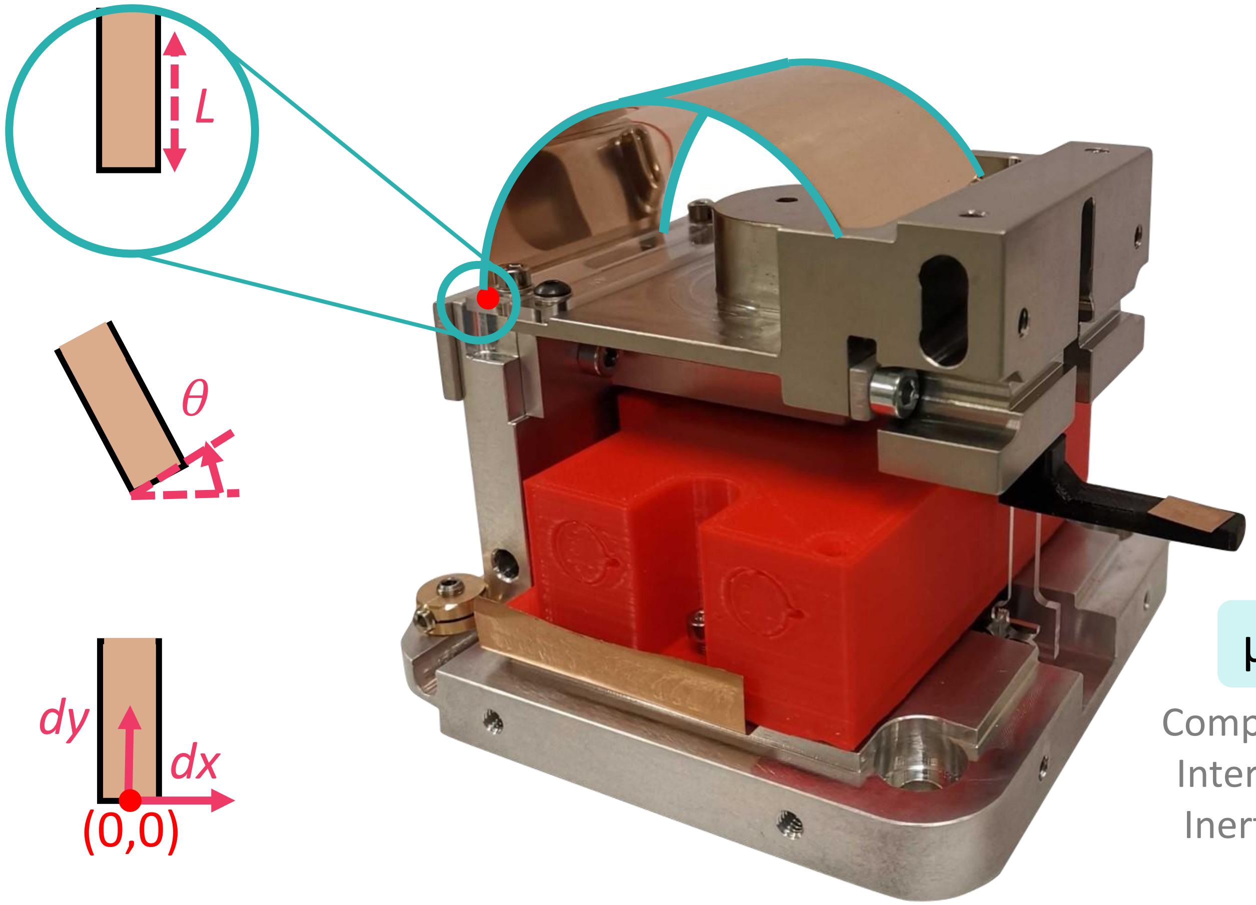

µVINS

Compact Vertical Interferometric Inertial Sensor

µVINS & studied parameters

$$f_0 = \frac{1}{2\pi}\sqrt{\frac{k}{m}}$$

Quasi-zero stiffness mechanism

Rotation

$$f_0^{(1)} = \frac{1}{2\pi}\sqrt{\frac{k_{LF} r_s^2 + \kappa_{flex}}{I}}$$

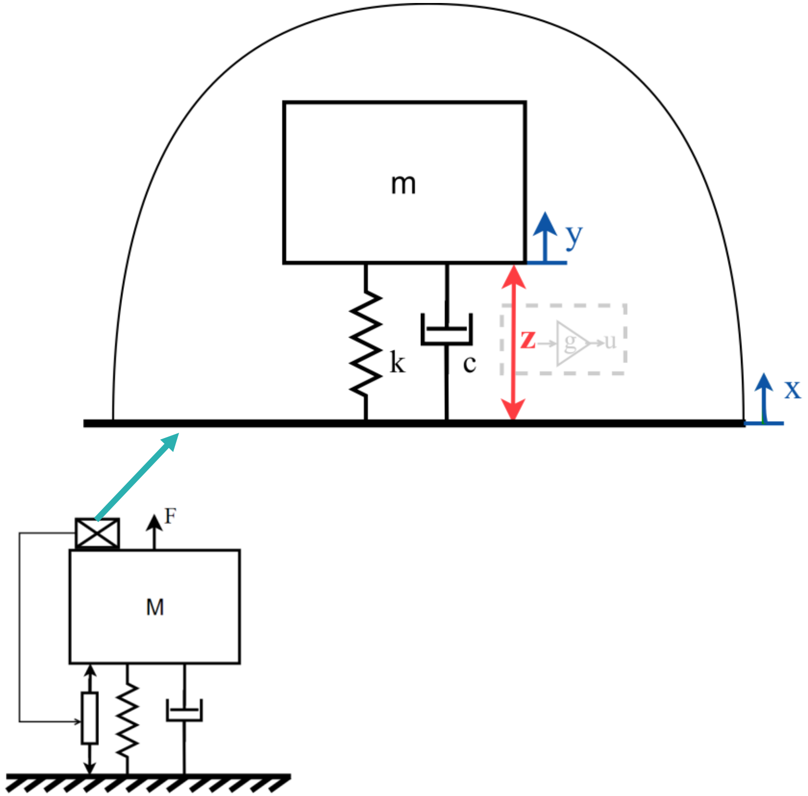

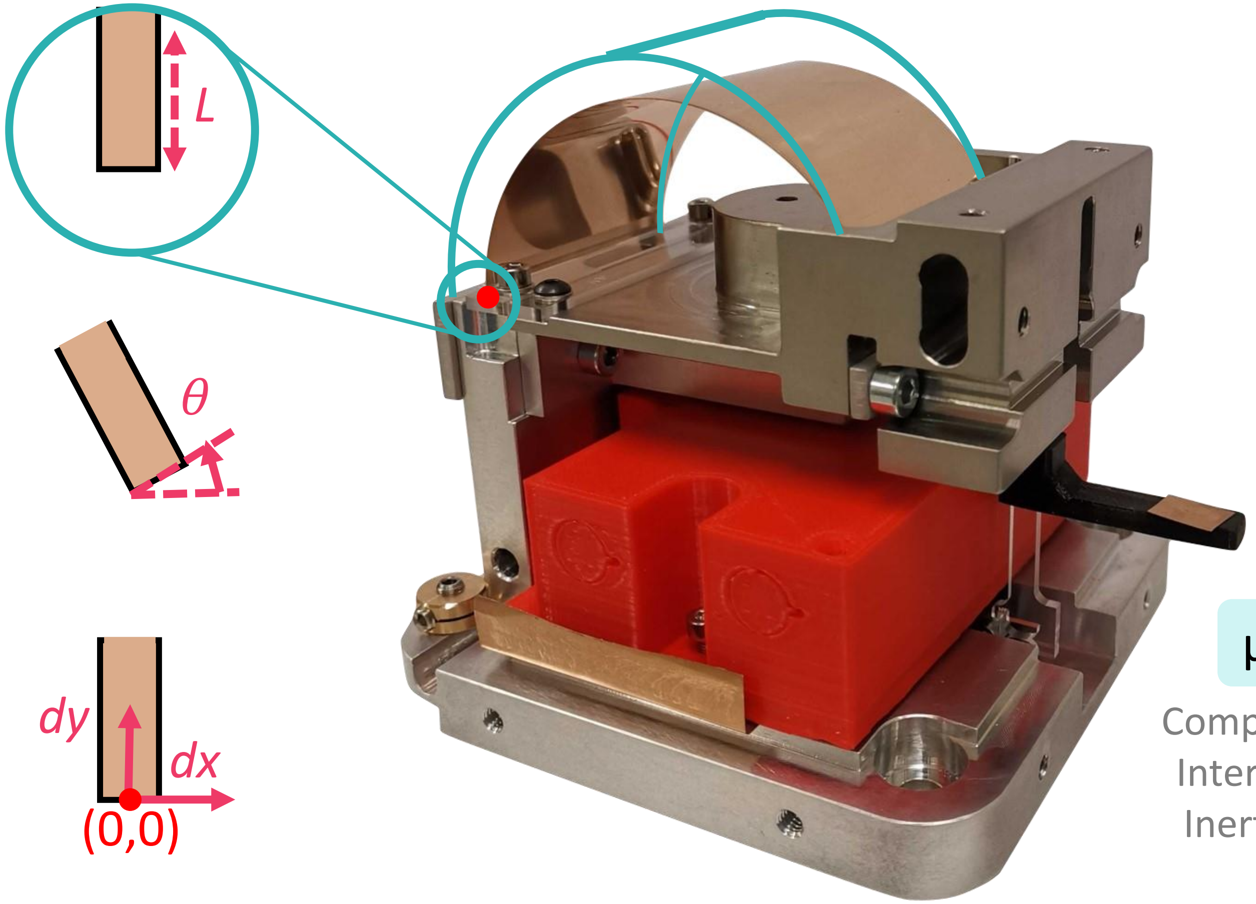

µVINS

Compact Vertical Interferometric Inertial Sensor

Methodology

Numerical tests

Experimental tests

Python software developed by the Aerospace & Mechanical Engineering department from ULiège

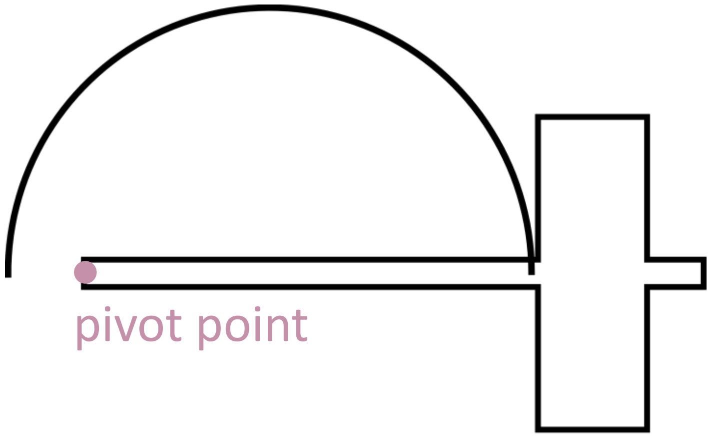

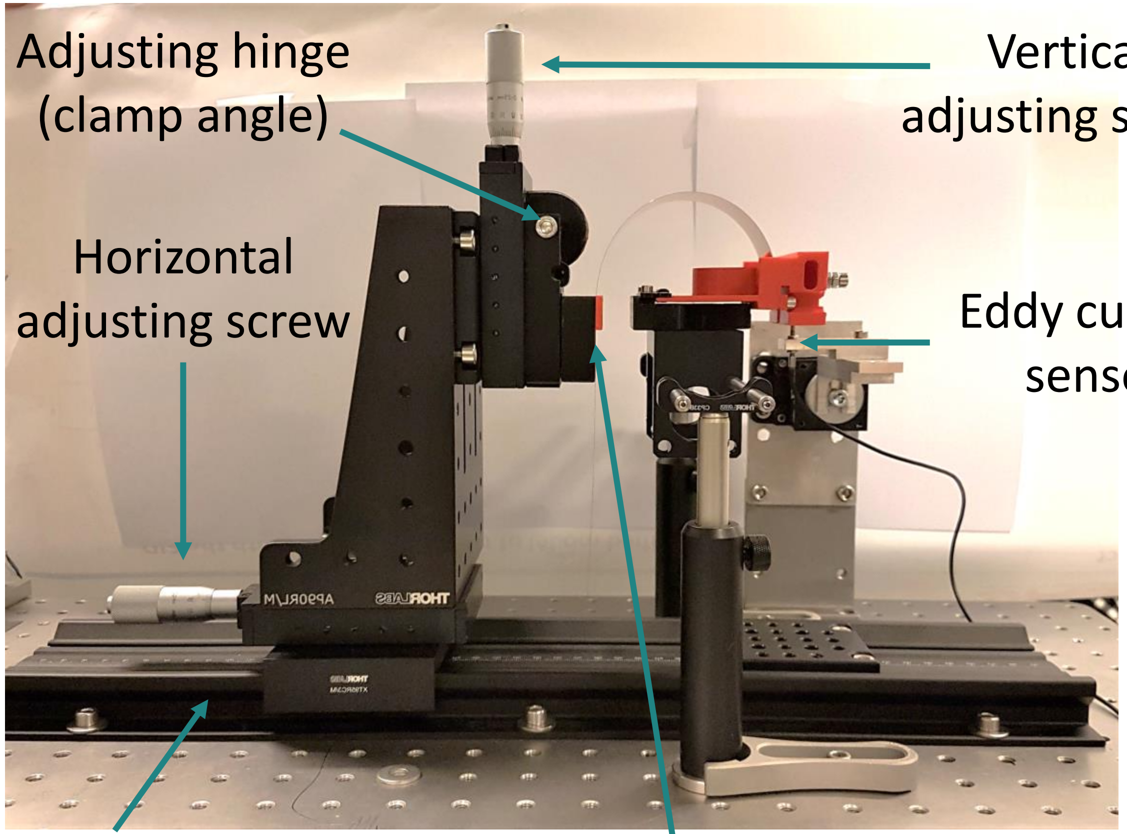

Locus of the points for which equilibrium is reached

L fix, ***dx*** and ***dy*** vary

= 1 configuration at equilibrium (boom horizontal)
= 1 simulation

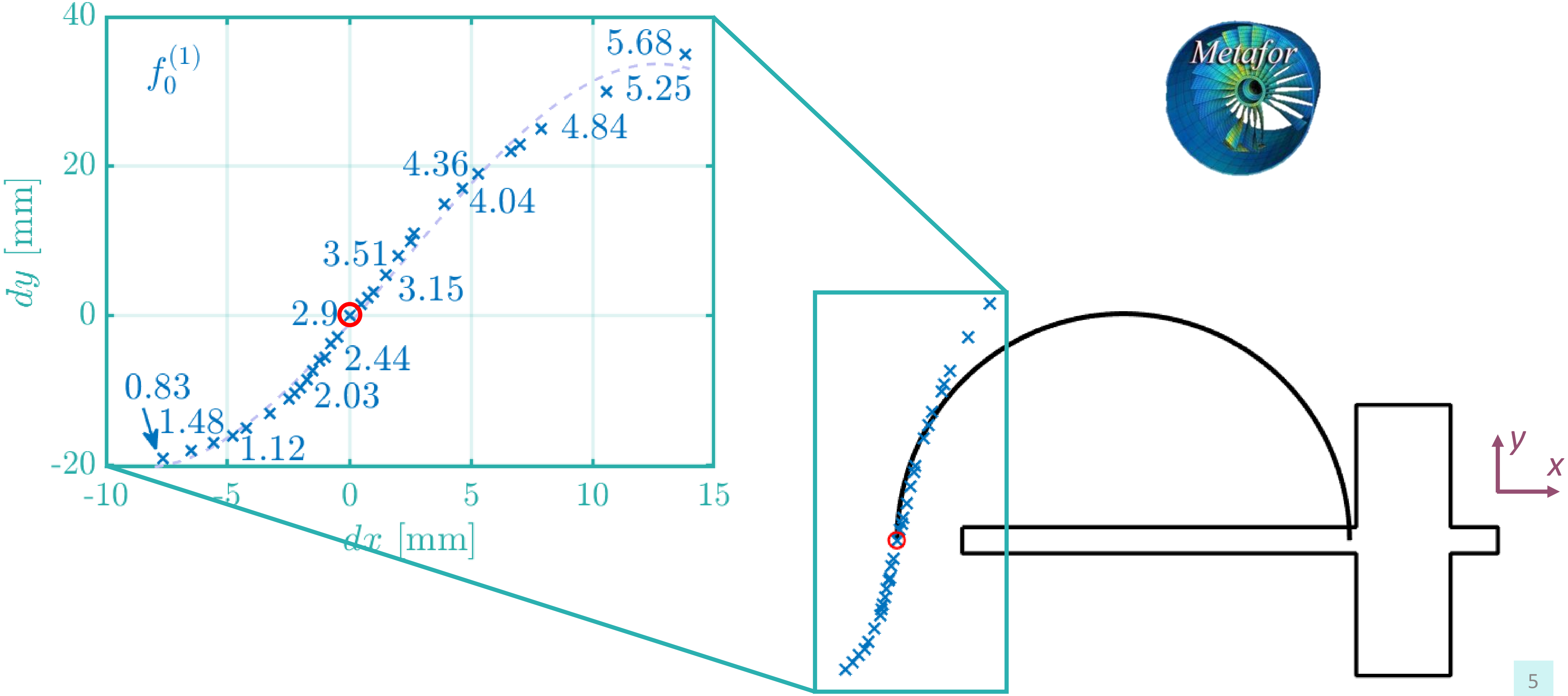

Resonance frequency

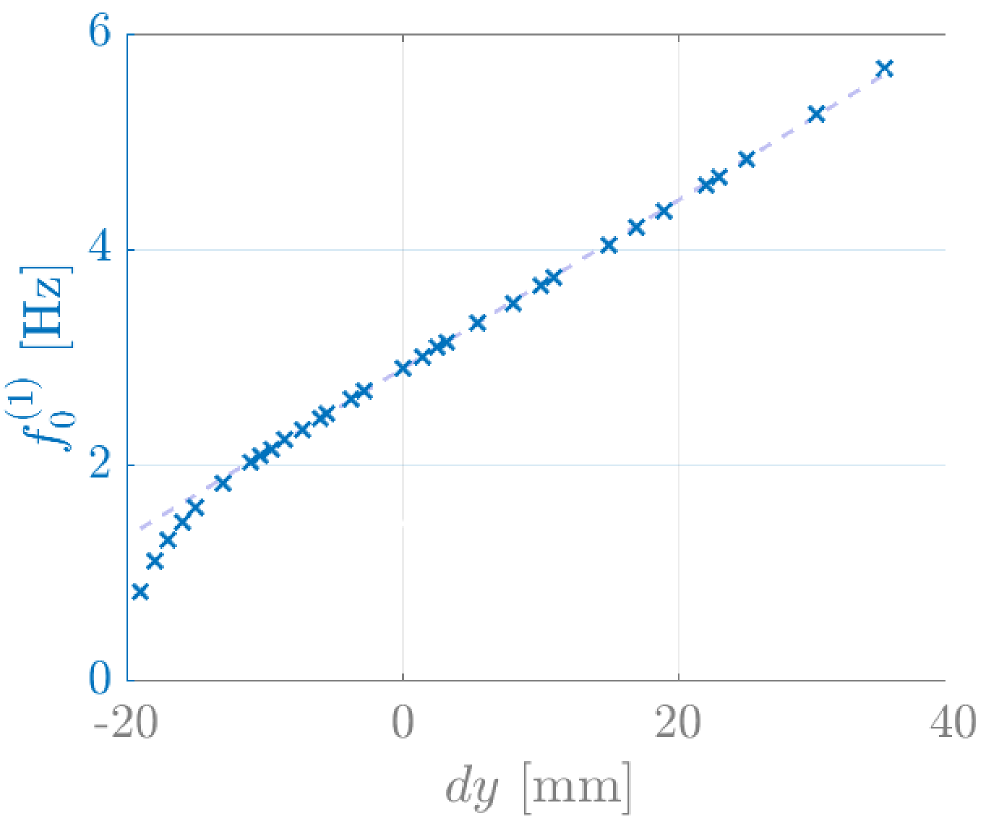

Resonance frequency

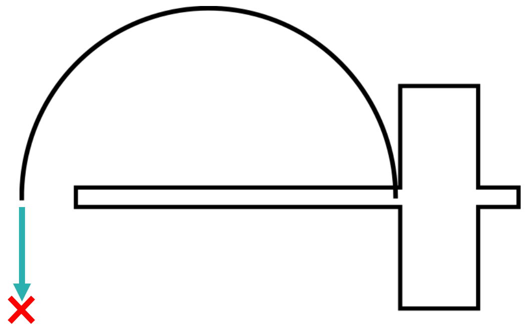

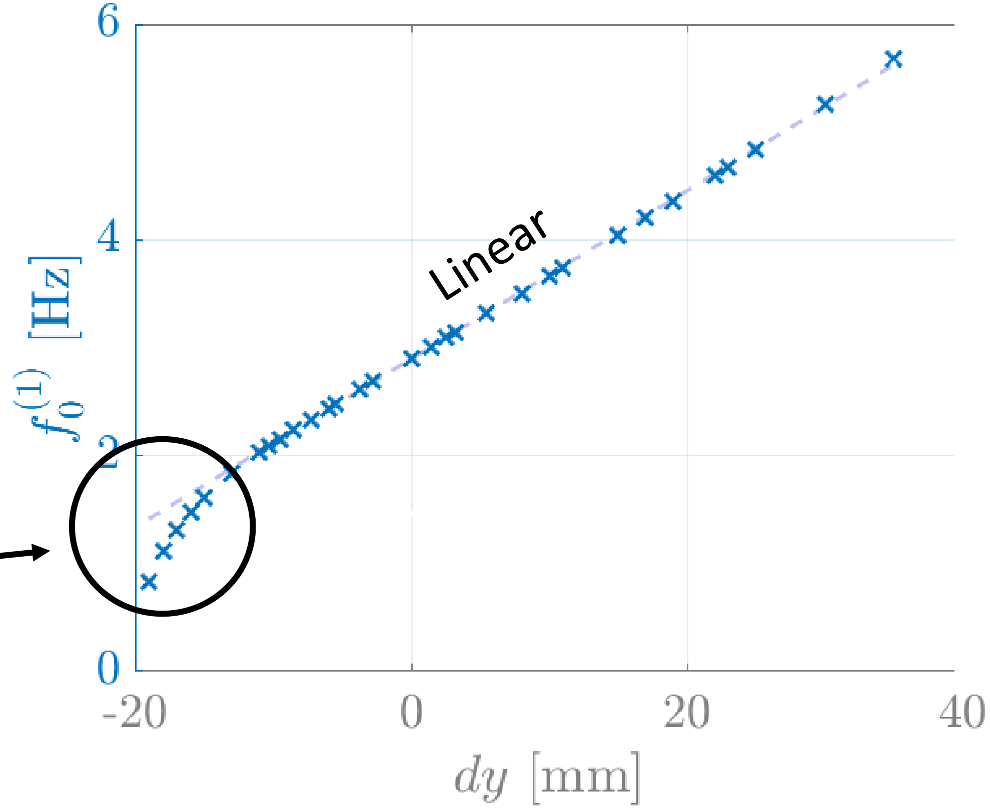

Dramatic drop of $f_0^{(1)}$

Instability point

Resonance frequency

$$f_0^{(1)} = \frac{1}{2\pi}\sqrt{\frac{k_{\mathrm{LF}} r_s^2 + \kappa_{\mathrm{flex}}}{I}}$$

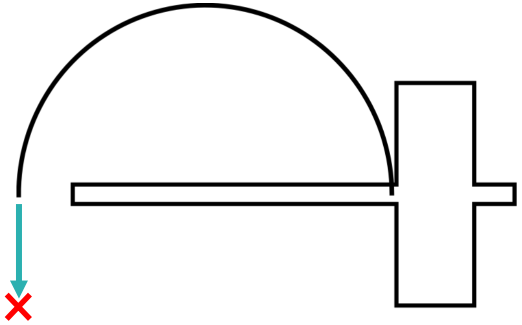

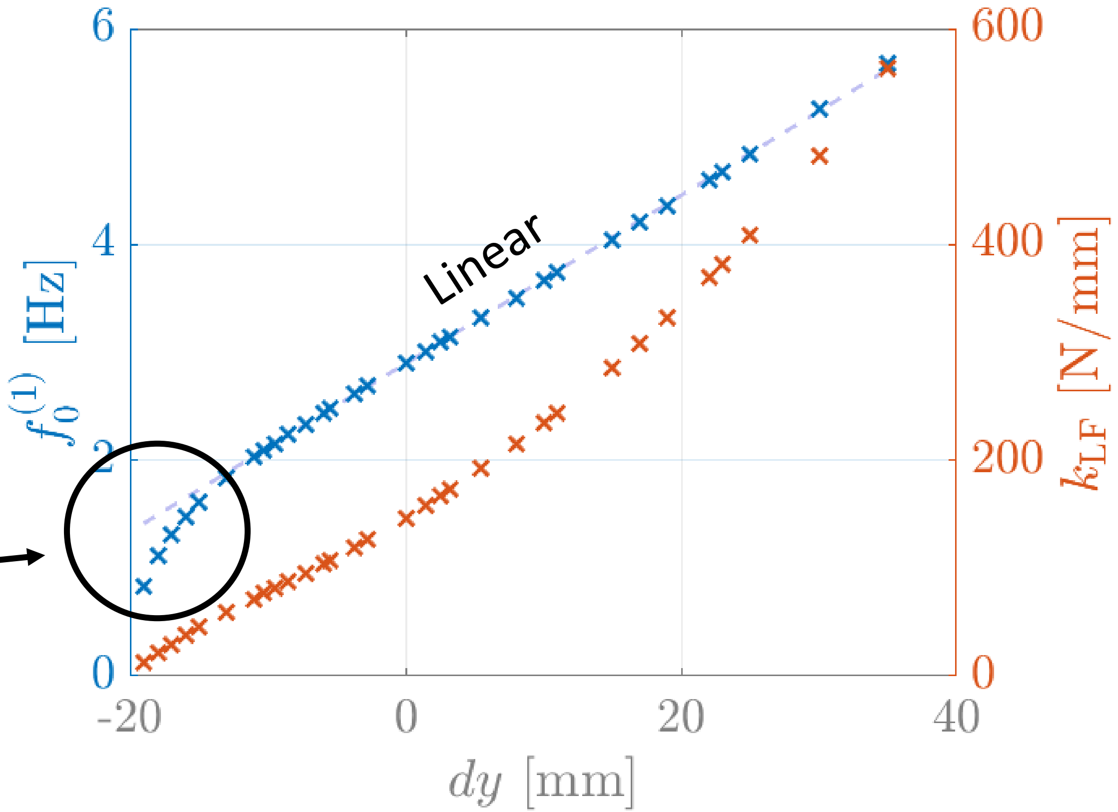

Dramatic drop of $f_0^{(1)}$

Instability point

Resonance frequency

$$f_0^{(1)} = \frac{1}{2\pi}\sqrt{\frac{k_{\mathrm{LF}} r_s^2 + \kappa_{\mathrm{flex}}}{I}}$$

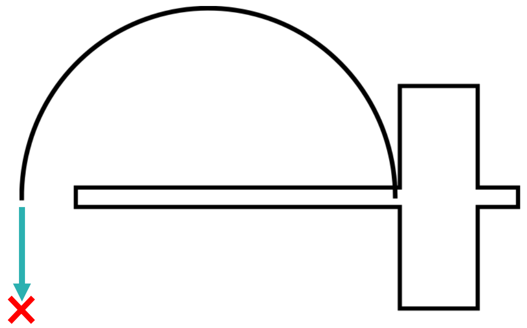

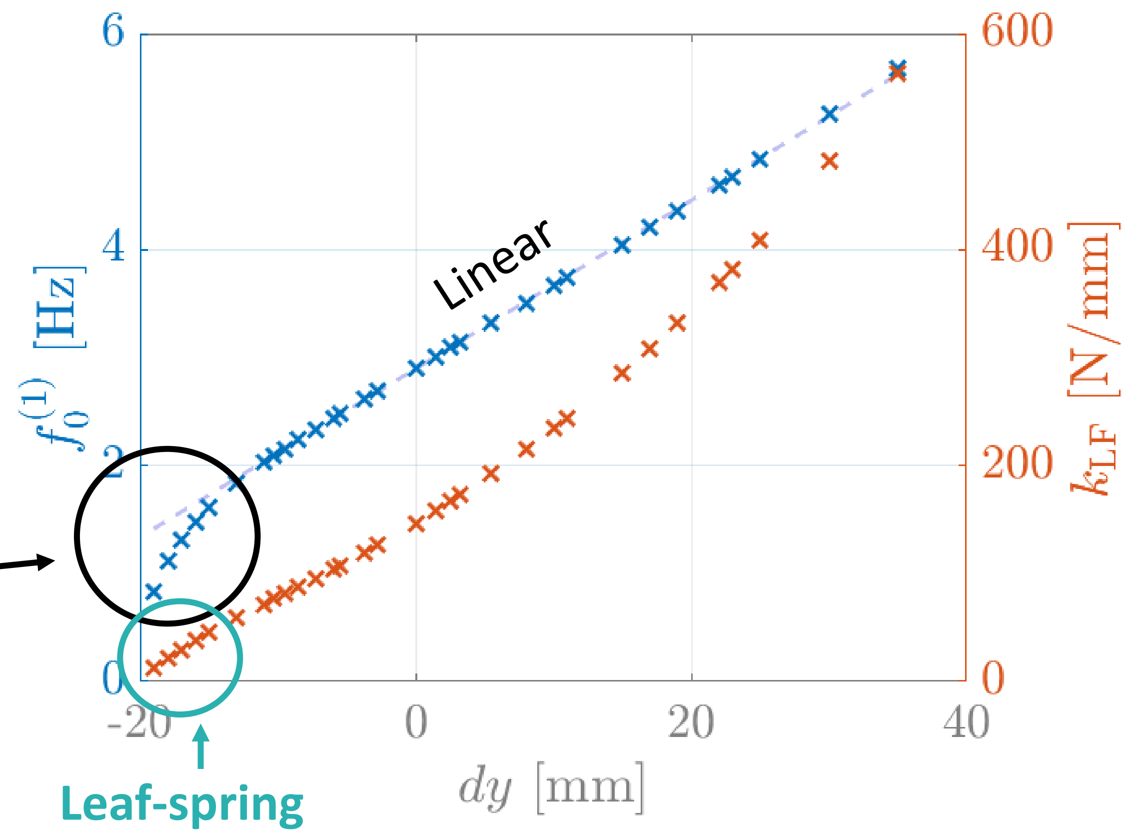

Dramatic drop of $f_0^{(1)}$

Instability point

Leaf-spring suspension

=

QZS mechanism

Resonance frequency

$$f_0^{(1)} = \frac{1}{2\pi}\sqrt{\frac{k_{\mathrm{LF}} r_s^2 + \kappa_{\mathrm{flex}}}{I}}$$

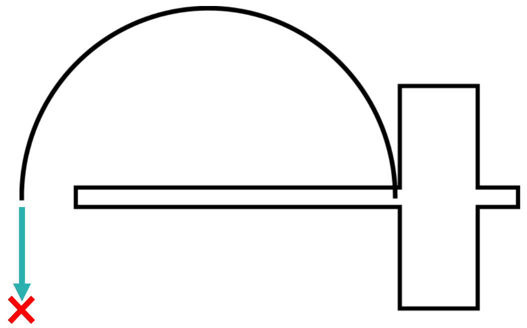

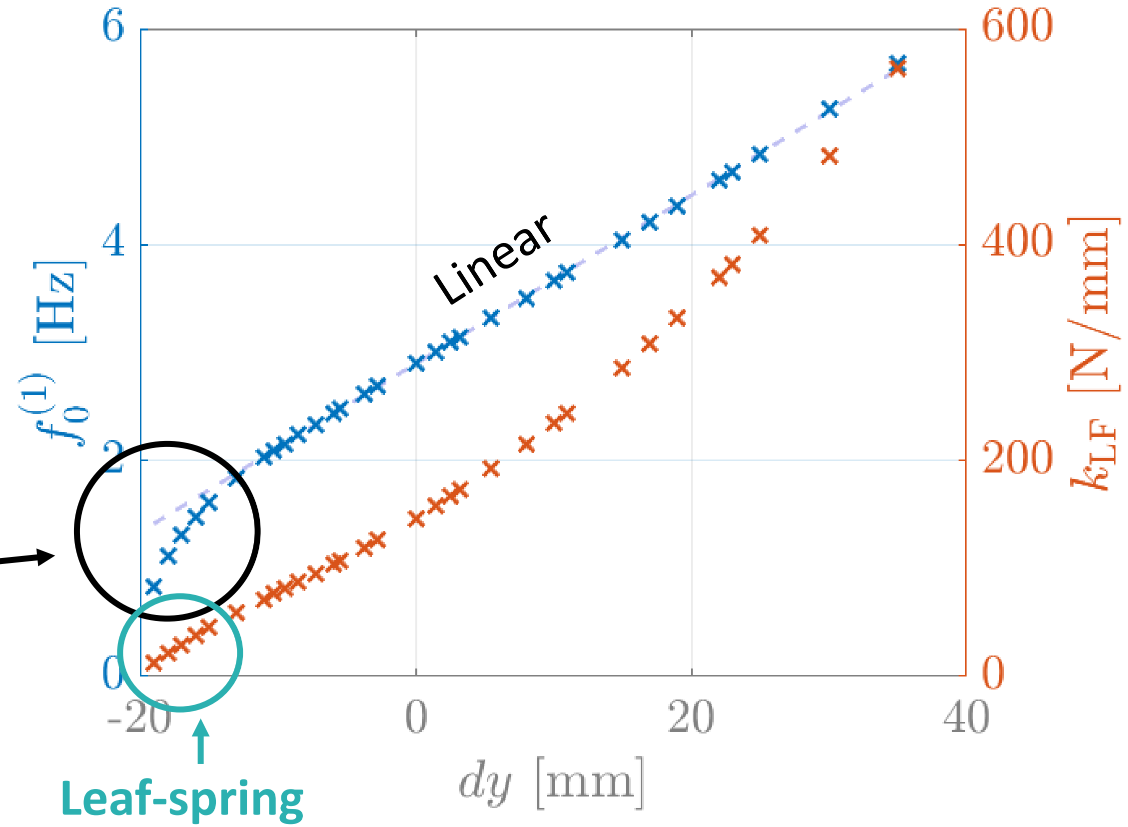

Dramatic drop of $f_0^{(1)}$

Instability point

Leaf-spring suspension = QZS mechanism

dy has the strongest impact on $f_0^{(1)}$

Shift clamping point **downward** to **decrease $f_0^{(1)}$**

Resonance frequency

$$f_0^{(1)} = \frac{1}{2\pi}\sqrt{\frac{k_{\mathrm{LF}} r_s^2 + \kappa_{\mathrm{flex}}}{I}}$$

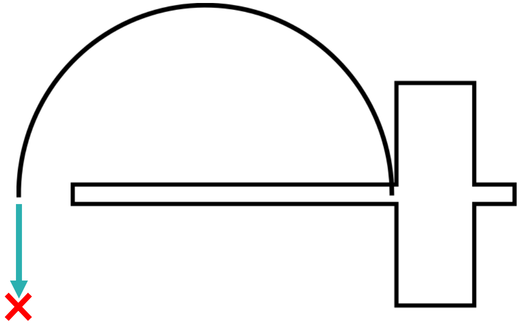

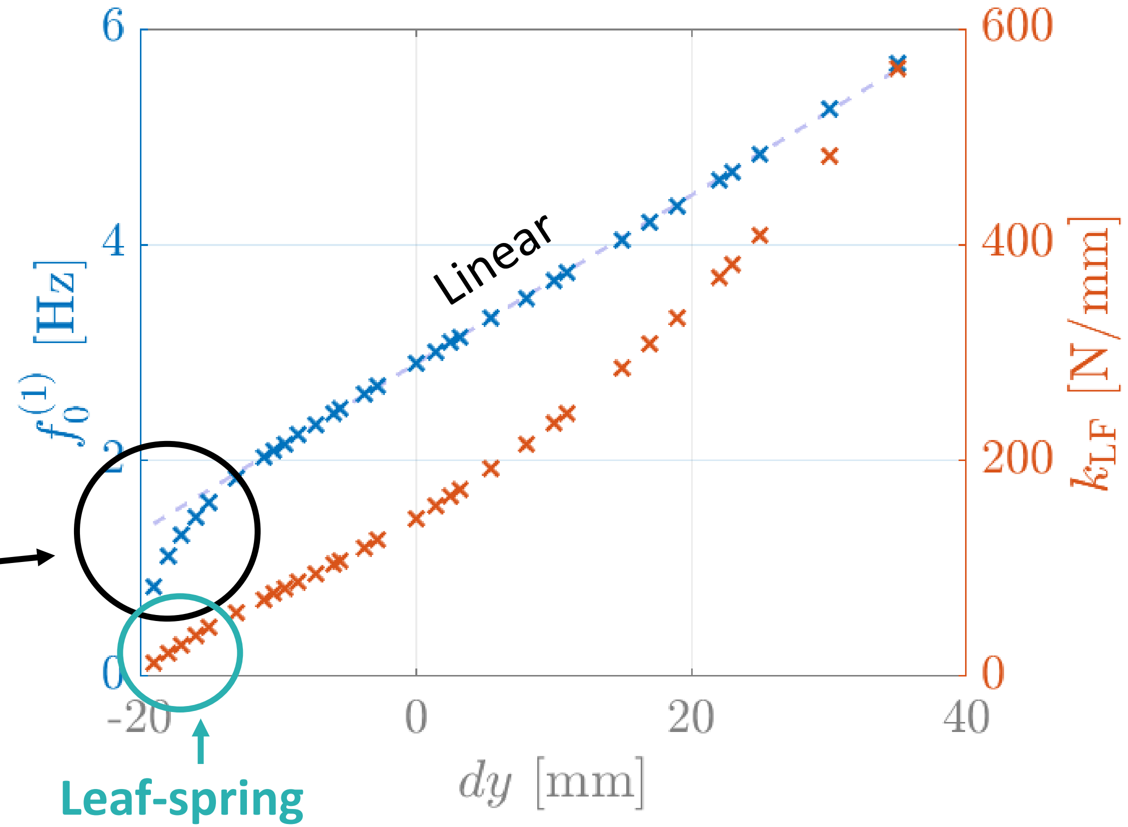

Dramatic drop of $f_0^{(1)}$

Instability point

Leaf-spring suspension

=

QZS mechanism

dy has the strongest impact on $f_0^{(1)}$

Shift clamping point **downward** to **decrease $f_0^{(1)}$**

dx has the strongest impact on the restoring moment

dx is used to guarantee the **equilibrium**

Leaf-spring length parameter

- Plastic mass & hinge
- *L* fixed & *dx* and *dy* variable → repetition for several *L*

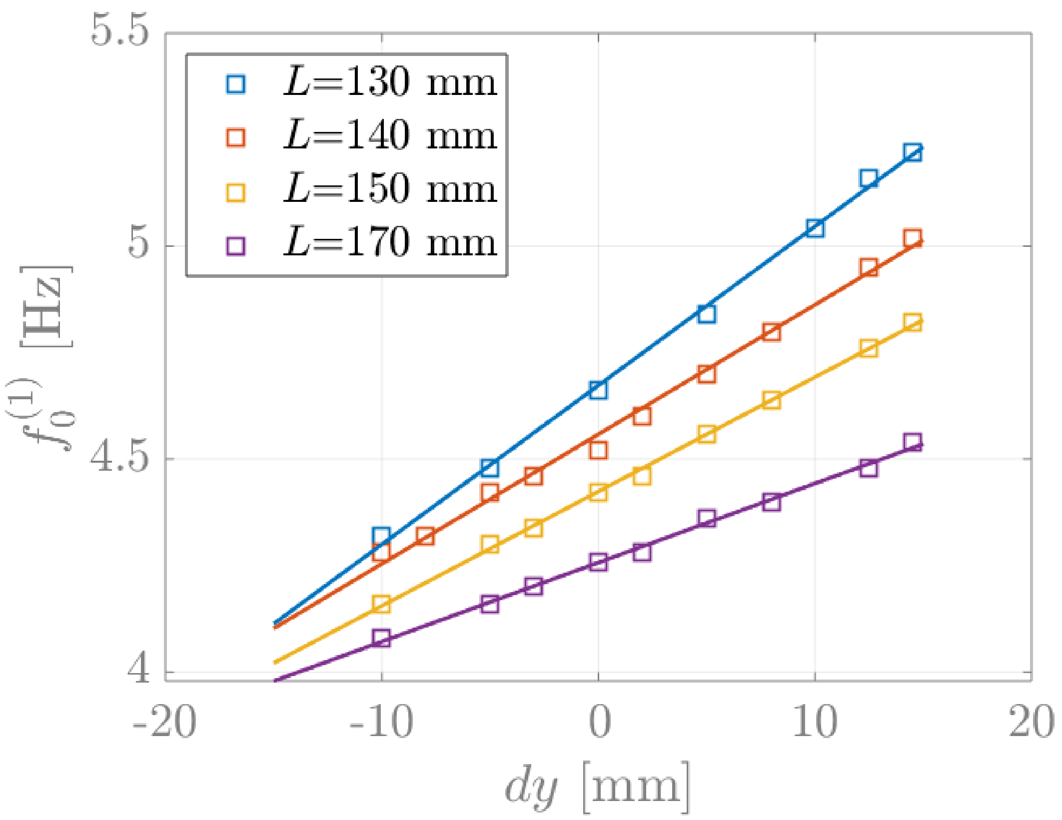

Leaf-spring length parameter

- Plastic mass & hinge
- *L* fixed & *dx* and *dy* variable → repetition for several *L*

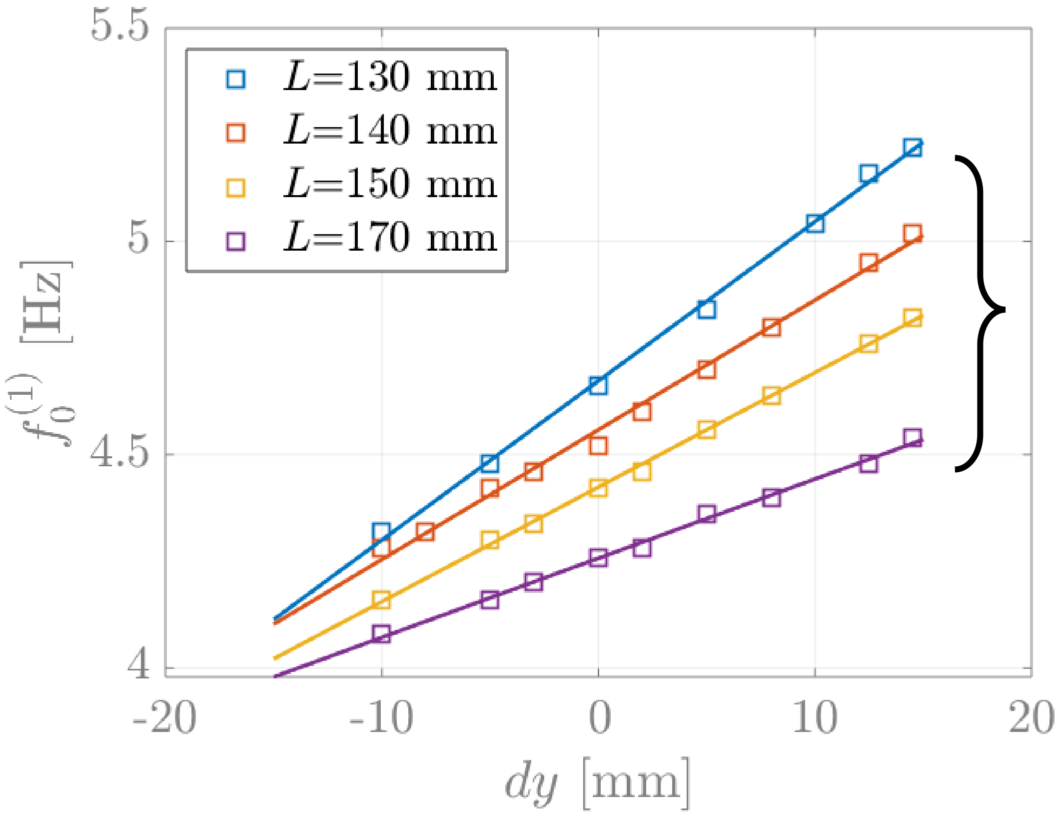

A longer leaf-spring attenuates the impact of *dy* (lower variation range for larger *L*)

Leaf-spring length parameter

- Plastic mass & hinge
- *L* fixed & *dx* and *dy* variable → repetition for several *L*

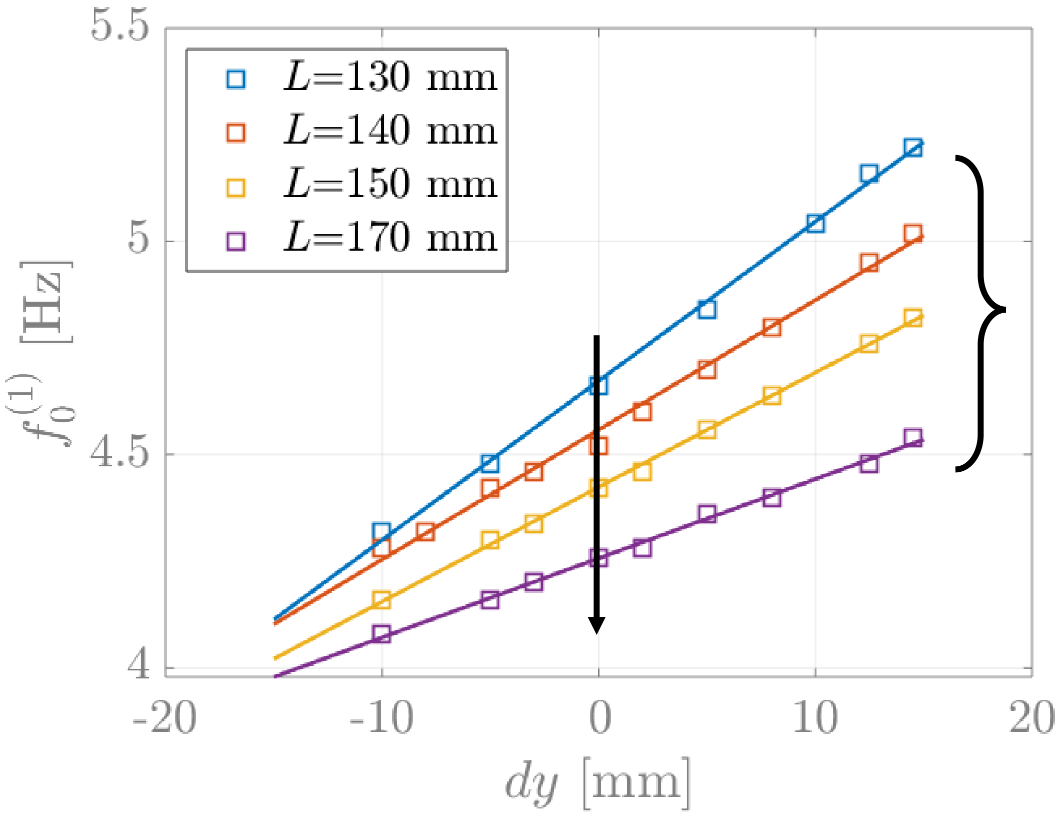

A longer leaf-spring attenuates the impact of *dy* (lower variation range for larger *L*)

Initial $f_0^{(1)}$ value decreases as *L* is increased

Leaf-spring length parameter

- Plastic mass & hinge
- *L* fixed & *dx* and *dy* variable → repetition for several *L*

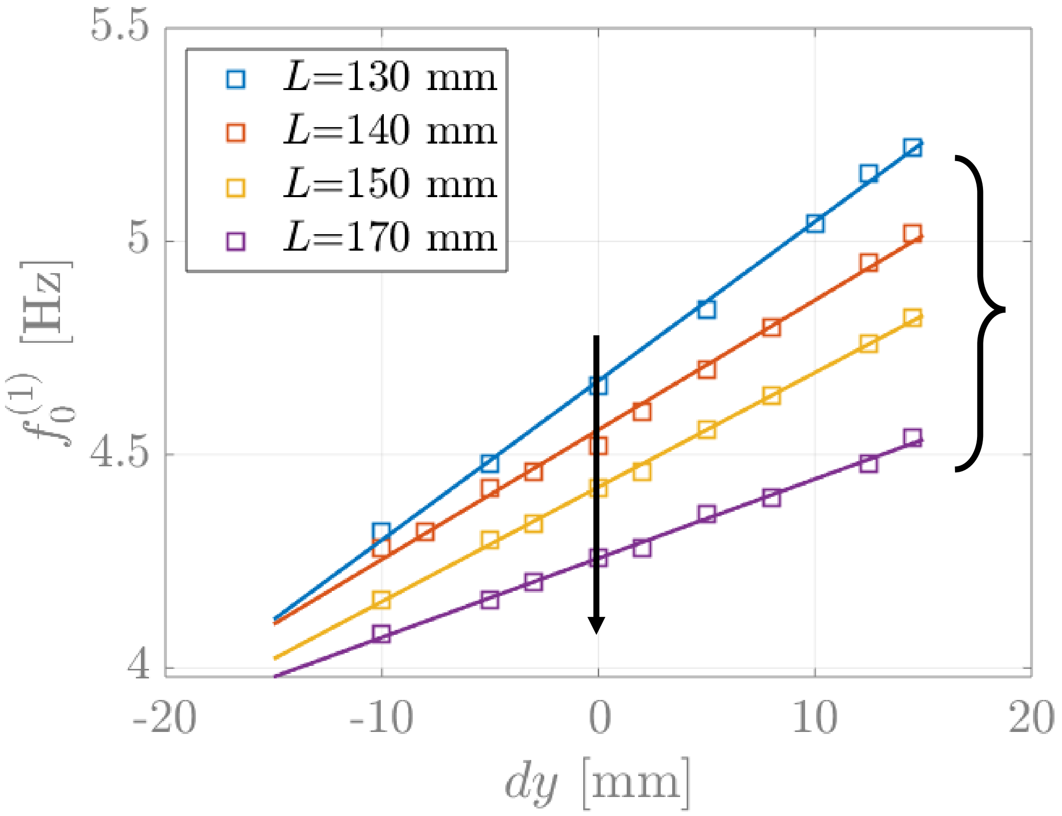

A longer leaf-spring attenuates the impact of *dy* (lower variation range for larger *L*)

Initial $f_0^{(1)}$ value decreases as *L* is increased

Trade-off

Clamping rotation parameter

- Steel mass (µVINS) & $CuBe_2$ hinge
- *L* and θ fixed & *dx* and *dy* variable → repetition for several θ

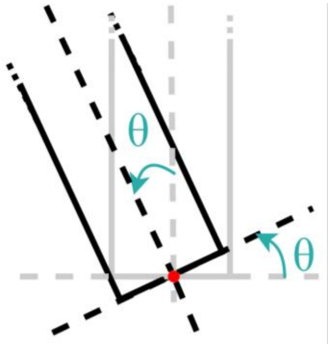

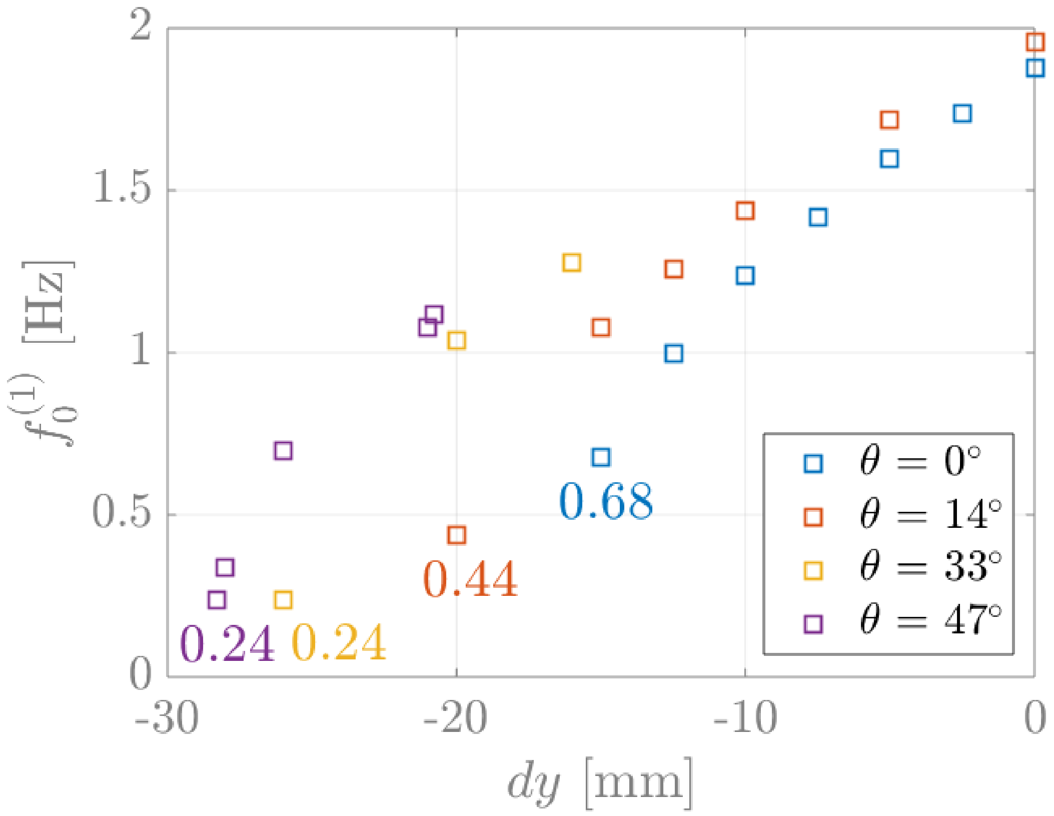

Clamping rotation parameter

- Steel mass (μVINS) & $CuBe_2$ hinge
- *L* and θ fixed & *dx* and *dy* variable → repetition for several θ

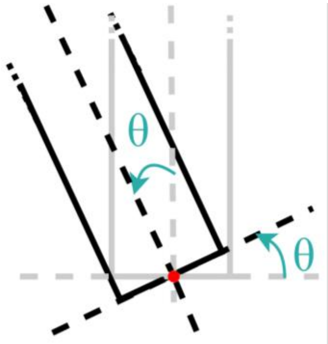

Increasing θ delays the frequency drop

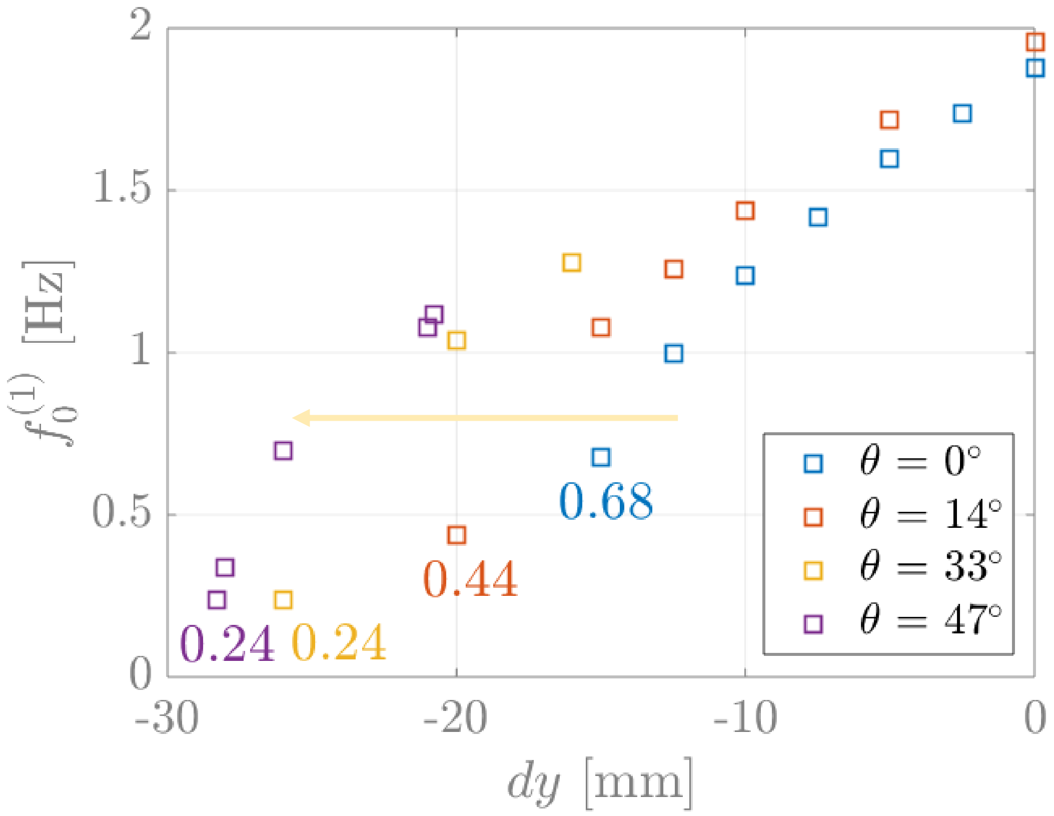

Clamping rotation parameter

- Steel mass (µVINS) & $CuBe_2$ hinge
- *L* and θ fixed & *dx* and *dy* variable → repetition for several θ

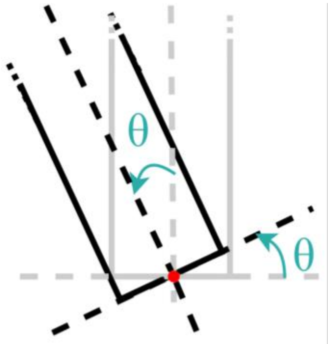

Increasing θ delays the frequency drop

The instability point occurs at lower *dy*

Decrease of $f_0^{(1)}$

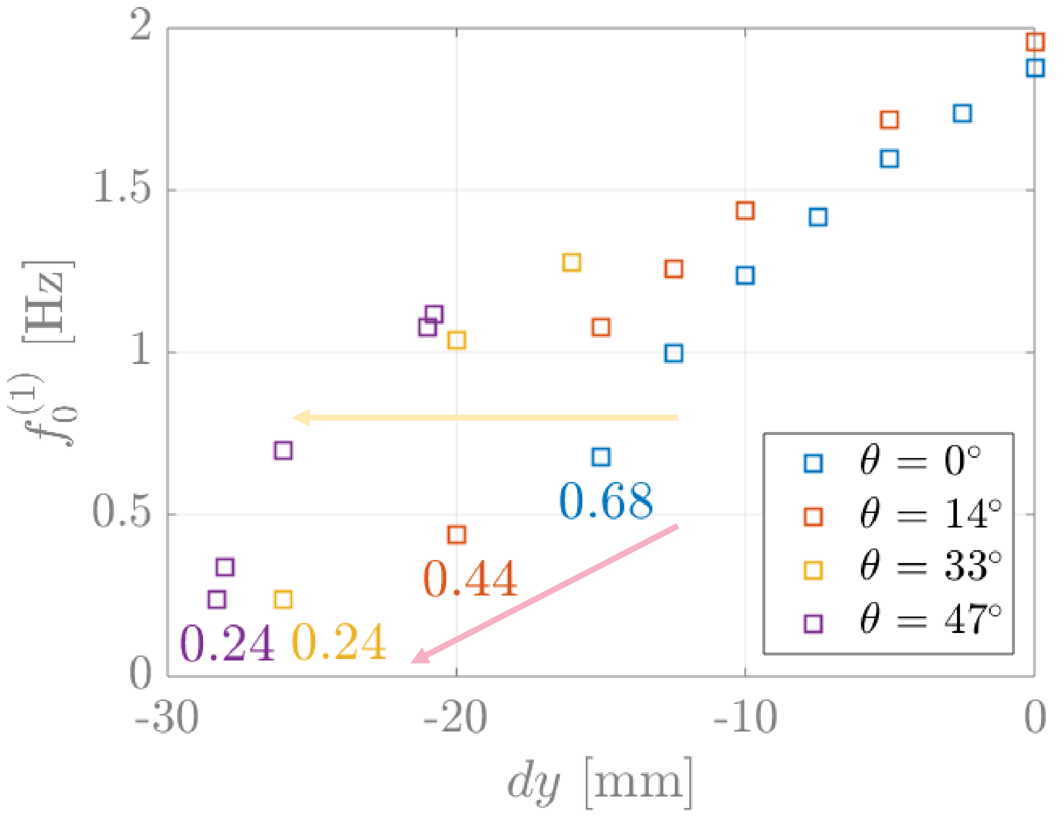

Clamping rotation parameter

- Steel mass (µVINS) & $CuBe_2$ hinge
- *L* and θ fixed & *dx* and *dy* variable → repetition for several θ

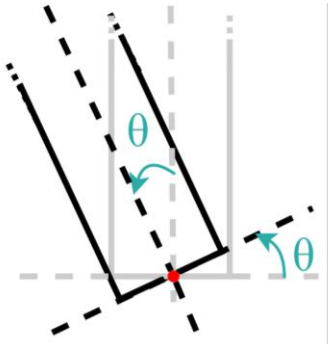

Increasing θ delays the frequency drop

The instability point occurs at lower *dy*

Decrease of $f_0^{(1)}$

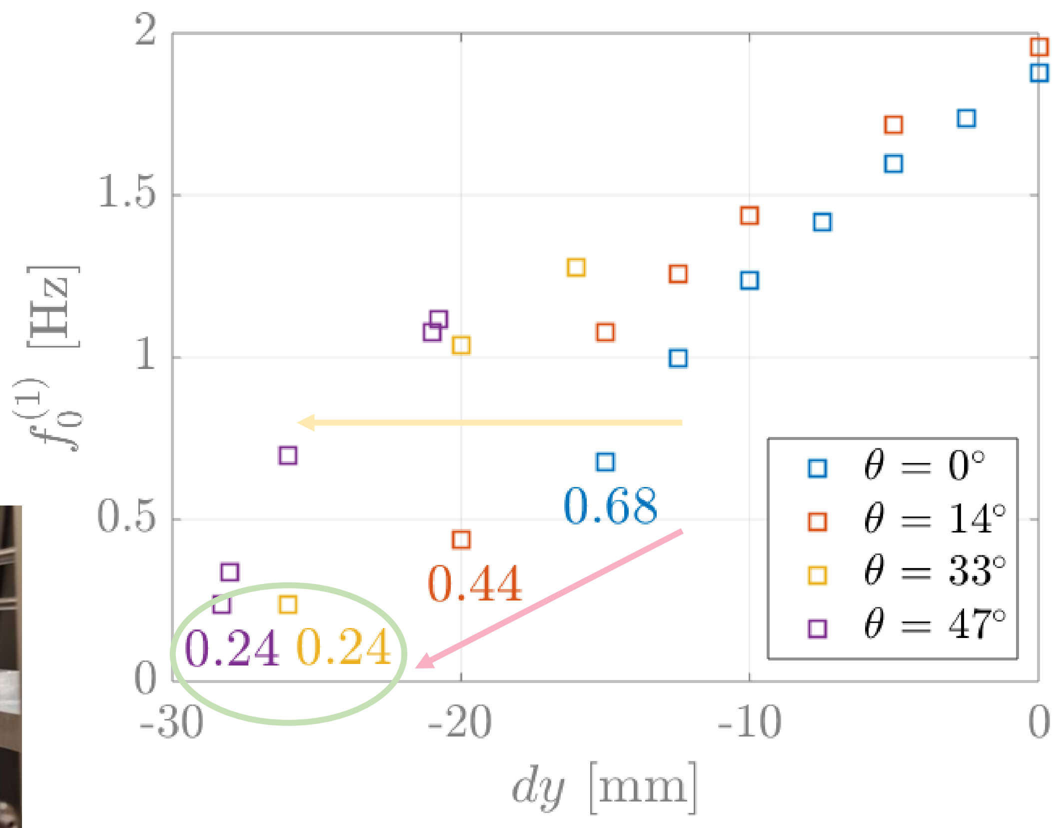

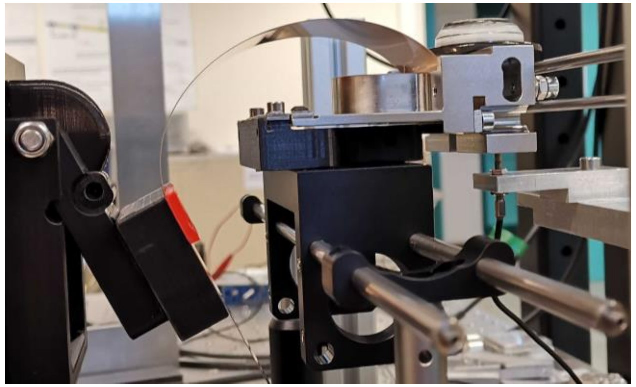

Above a given angle, $f_0^{(1)}$ does not decrease anymore but the internal stress increases

Clamping rotation parameter

- Steel mass (µVINS) & $CuBe_2$ hinge
- *L* and θ fixed & *dx* and *dy* variable → repetition for several θ

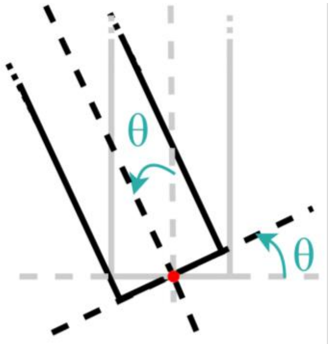

Increasing θ delays the frequency drop

The instability point occurs at lower *dy*

Decrease of $f_0^{(1)}$

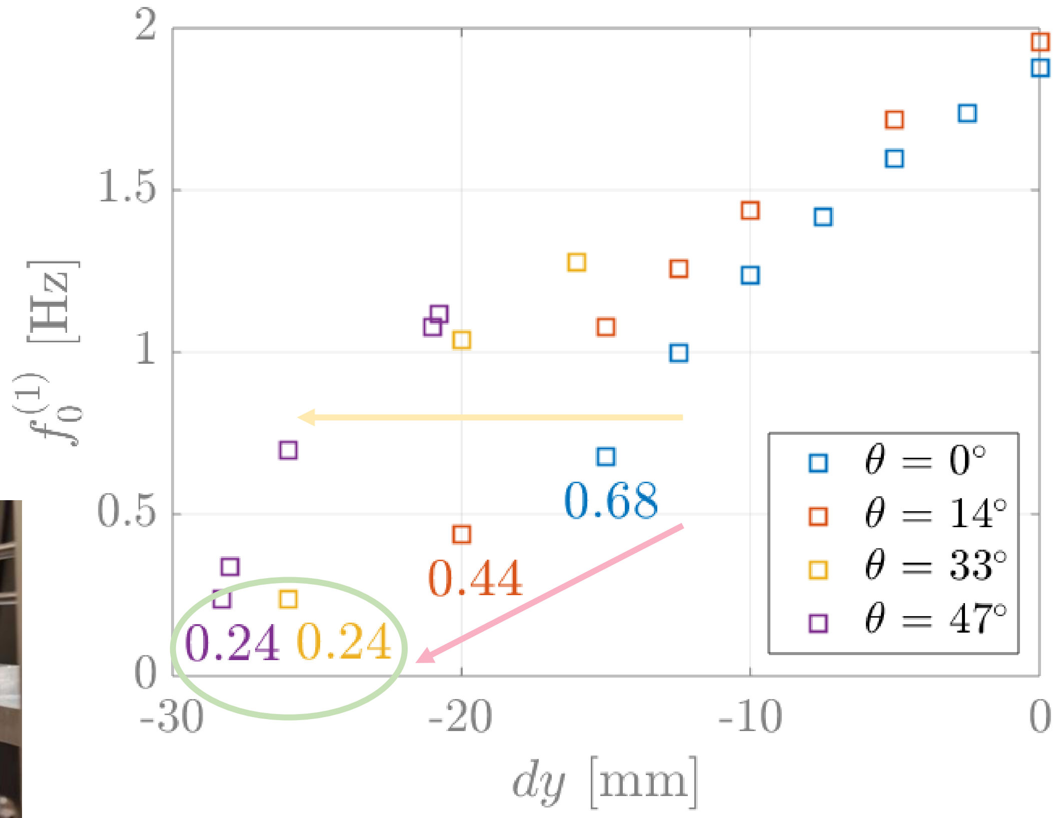

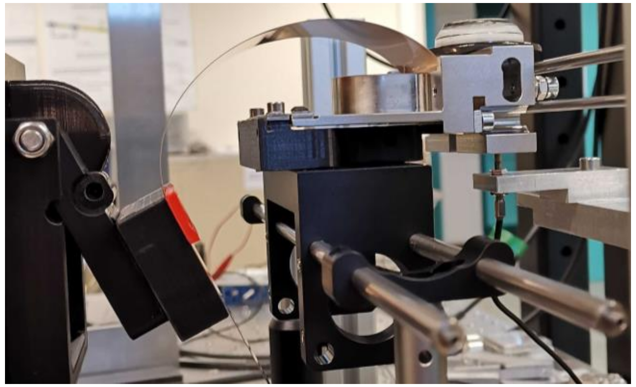

Above a given angle, $f_0^{(1)}$ does not decrease anymore but the internal stress increases

Optimal angle that minimizes $f_0^{(1)}$ and limit the internal stress

Conclusion & Design suggestion

The leaf-spring suspension can be tuned into a **Quasi-Zero Stiffness** mechanism

***dy* → $\boldsymbol{f_0^{(1)}}$**
Shift the clamping point downwards to decrease the sensor resonance frequency and thus widen the measurement bandwidth

θ → instability point
Optimum angle that gives the lowest $f_0^{(1)}$

***dx* → restoring moment**
Guarantees the sensor equilibrium

Trade-off on *L*
larger *L* lowers the initial resonance frequency but slows down its decrease

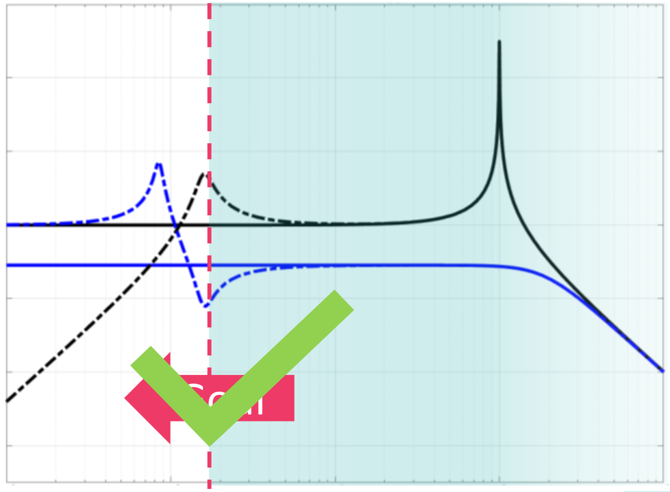

Reduction by **1 order of magnitude** of µVINS resonance frequency

Thank you for your attention!

Any questions?

Contact: morgane.zeoli@uclouvain.be

Additional slides

Design proposition

- Leaf-spring: 115 x 0.24 x 45 mm
- *dy* = -24.15 mm
- *dx* = -3.543 mm (ref: 17.78 mm)
- θ = 10°

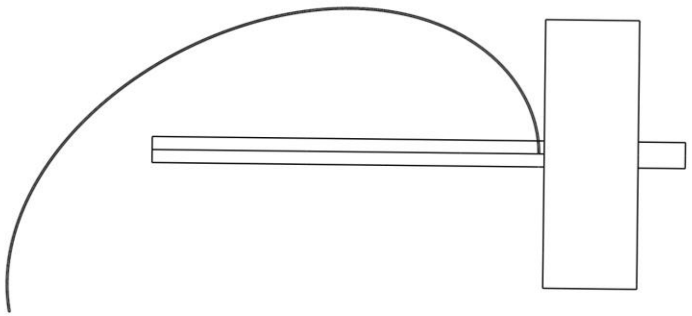

$f_0^{(1)} = 2.9\ \text{Hz}$
$f_0^{(2)} = 179.61\ \text{Hz}$

-2.76 Hz (-95.34%)

+7.04 Hz (+3.92%)

	µVINS	VINS	iSTS1	iSeis
$f_0^{(1)}$ [Hz]	**0.14**	0.26	0.19	0.39
$f_0^{(2)}$ [Hz]	**172.57**	-	-	-
Size [mm]	**104 x 104 x 103**	120 x 170 x 180		-

µVINS numerical modeling

Leaf-spring astatic suspension

Sensor ← $f_0^{(1)} = 2.9$ Hz → $\epsilon = 3.02\%$

Leaf-spring suspension ← $f_0^{(2)} = 179.61$ Hz

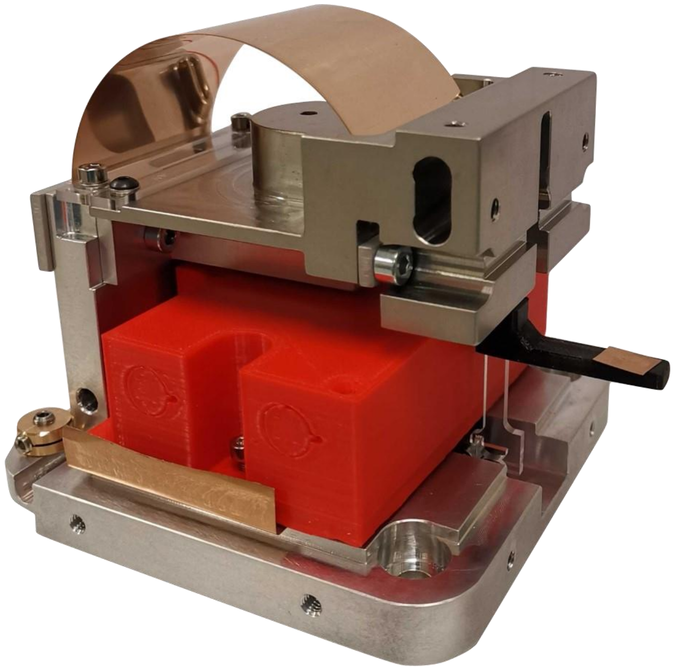

Total mass
CoM (r_1)
Radius r_2
Inertia

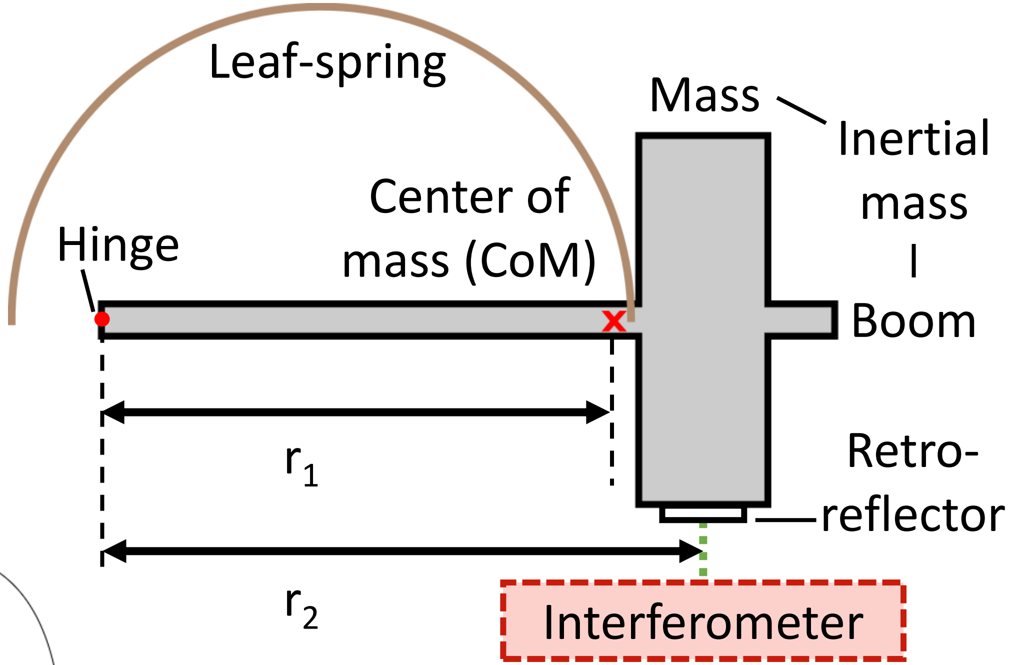

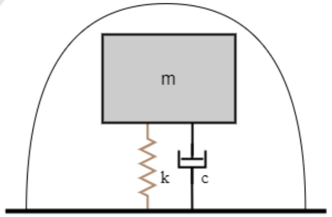

QZS mechanisms

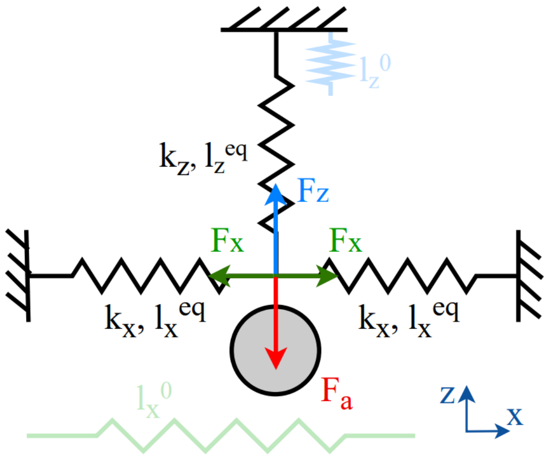

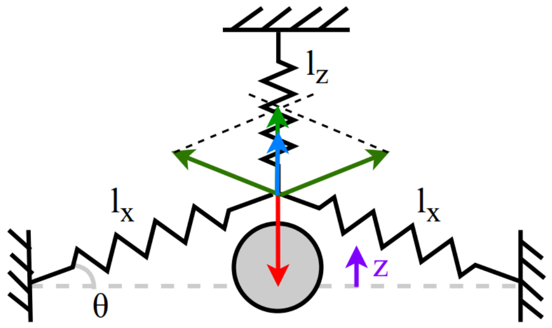

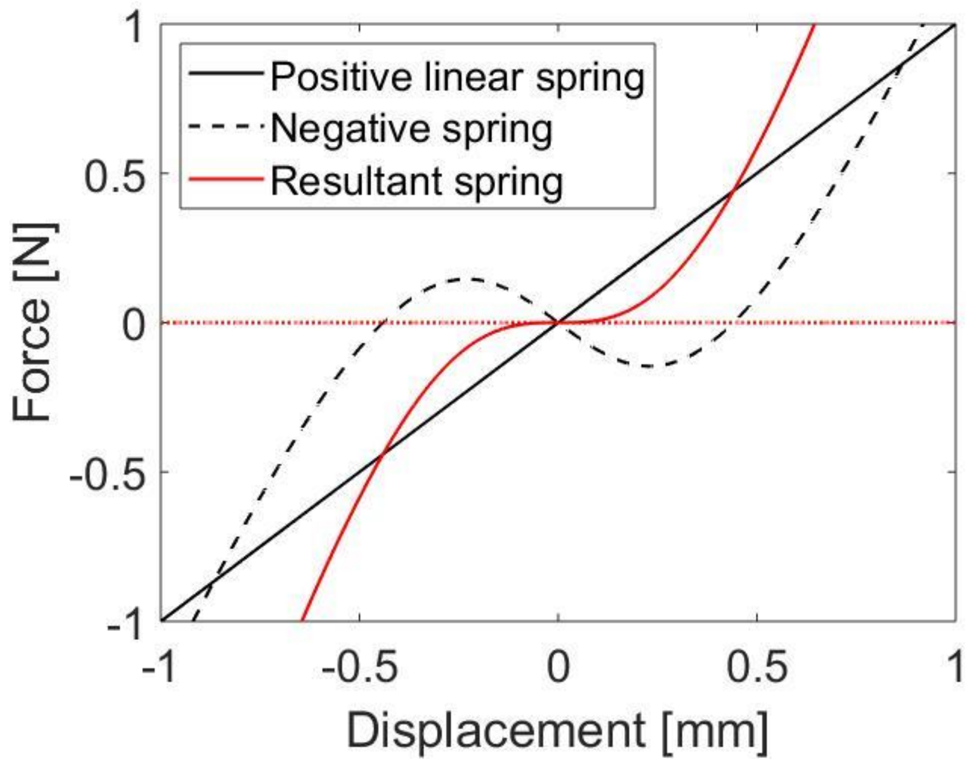

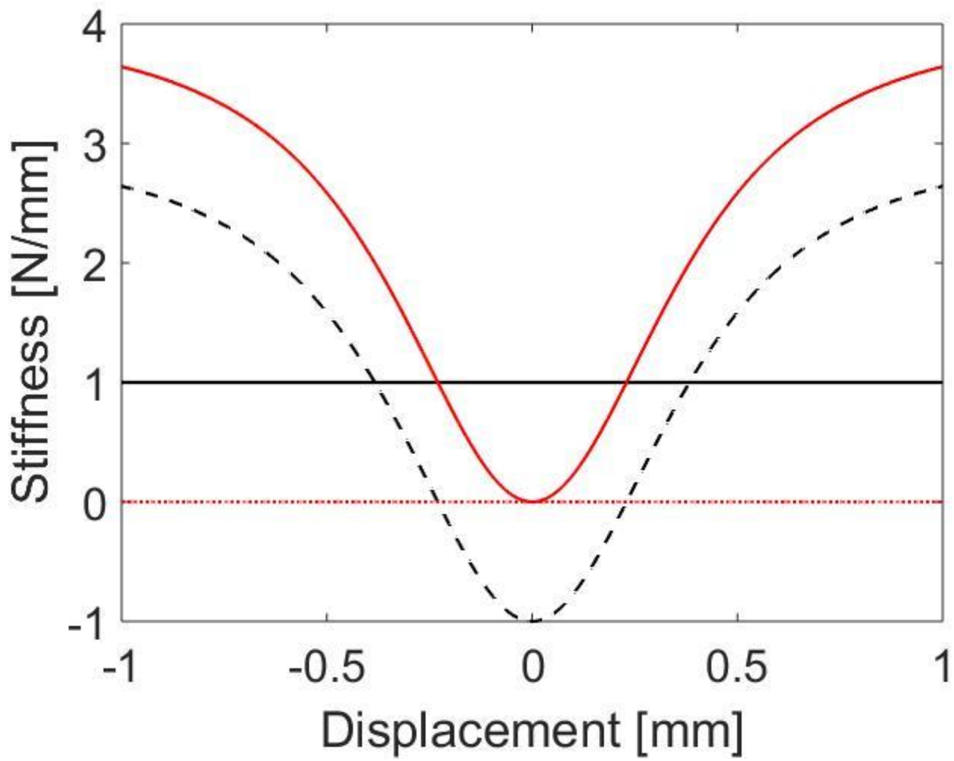

Influence of *dx*, *dy* and *L* – 1 fixed, 2 variable ($f_0^{(1)}$)

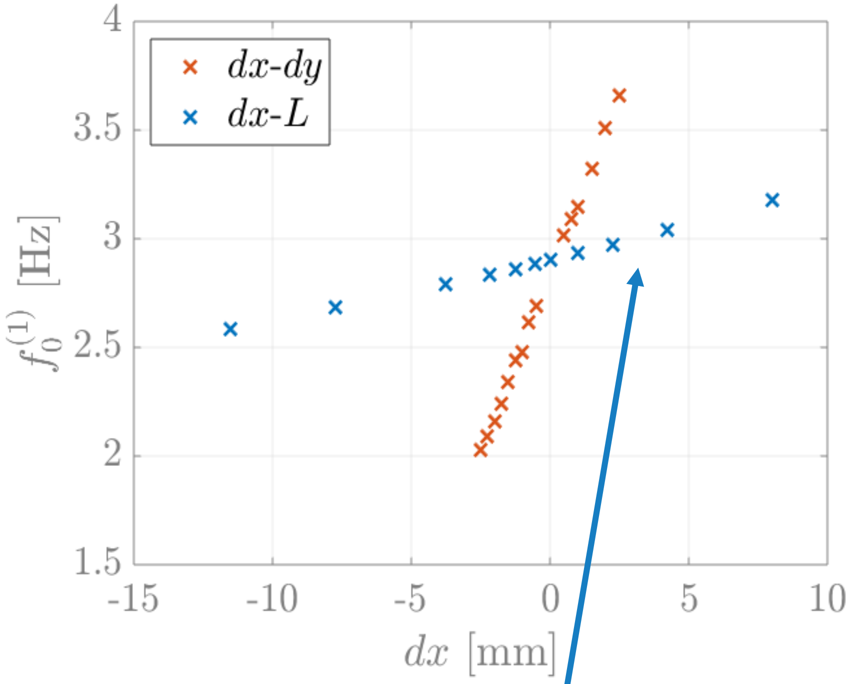

***dy* has the strongest impact on $f_0^{(1)}$**

Shift clamping point **downward** to **decrease** $f_0^{(1)}$

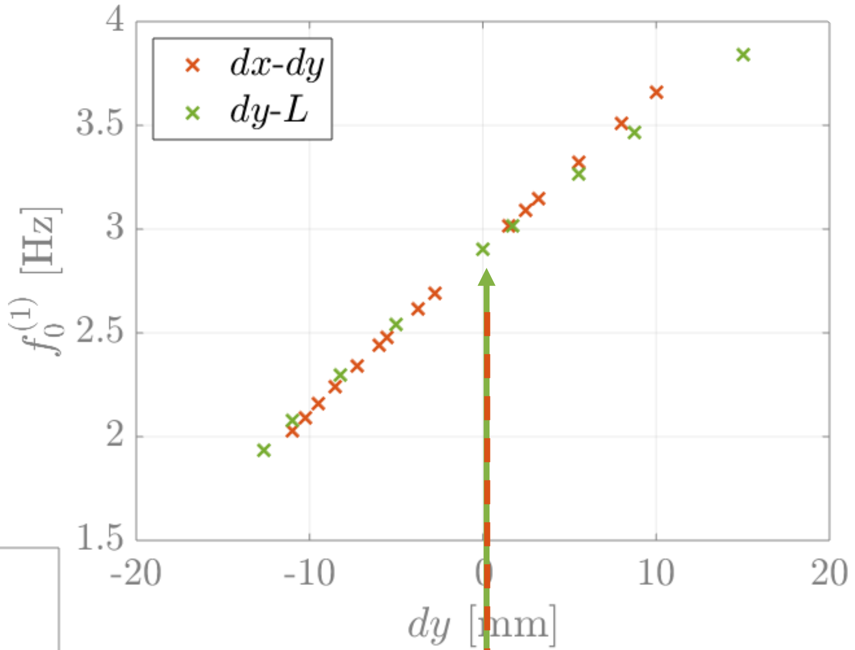

Lower variation range of $f_0^{(1)}$

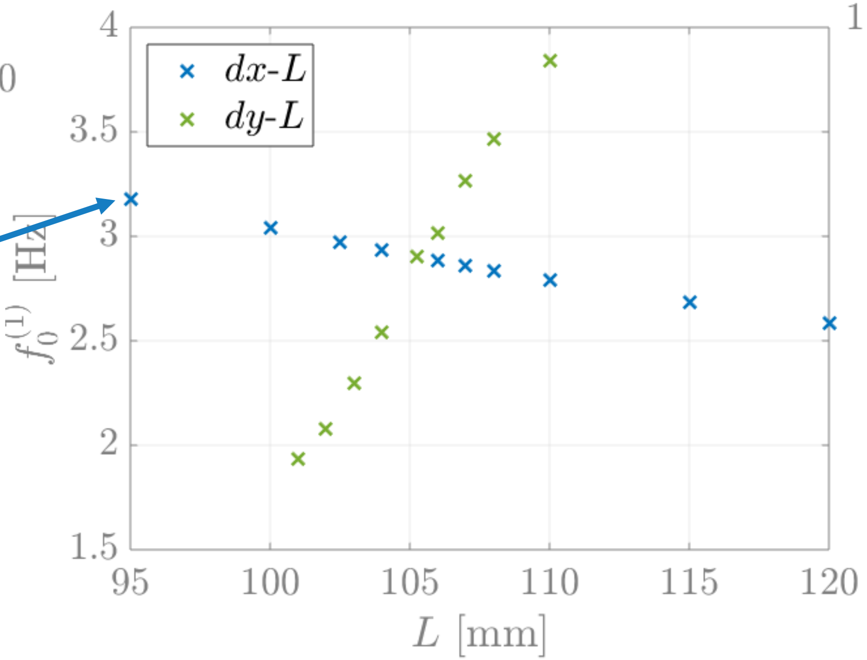

Curves very close: the effects of *dx* & *L* are lower than the one of *dy*

Influence of *dx*, *dy* and *L* – 1 fixed, 2 variable ($f_0^{(2)}$)

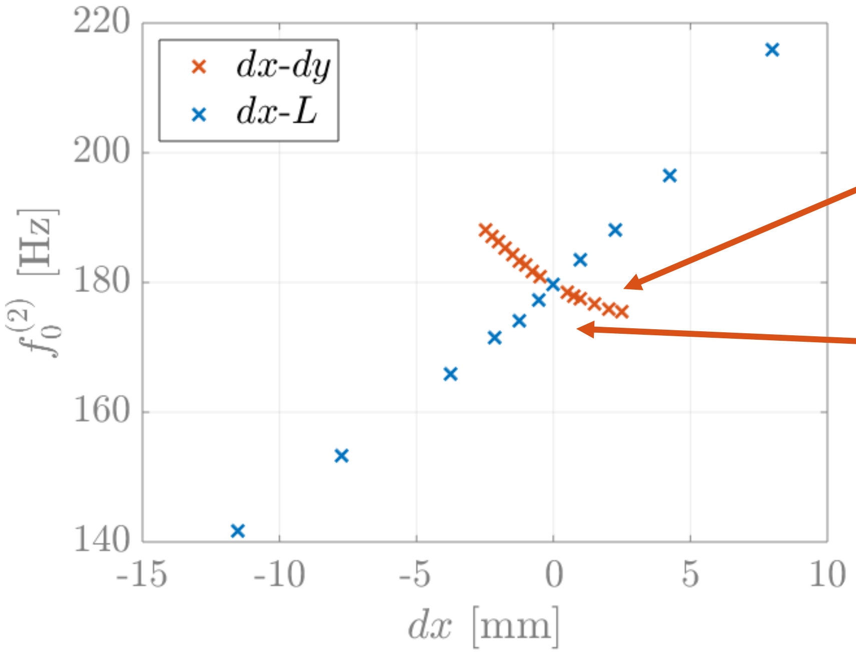

Lower variation range of $f_0^{(2)}$

L dominates the effect of *dx*

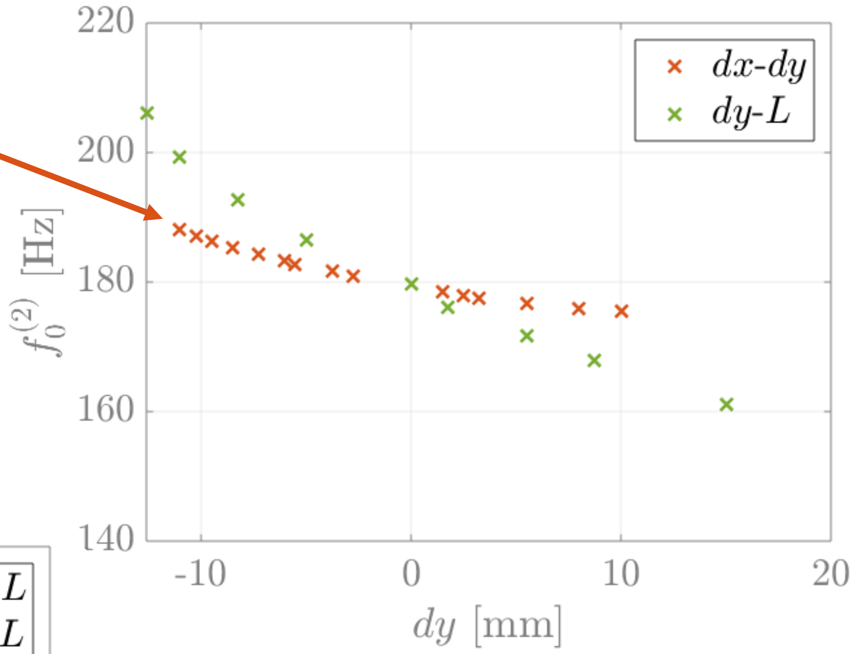

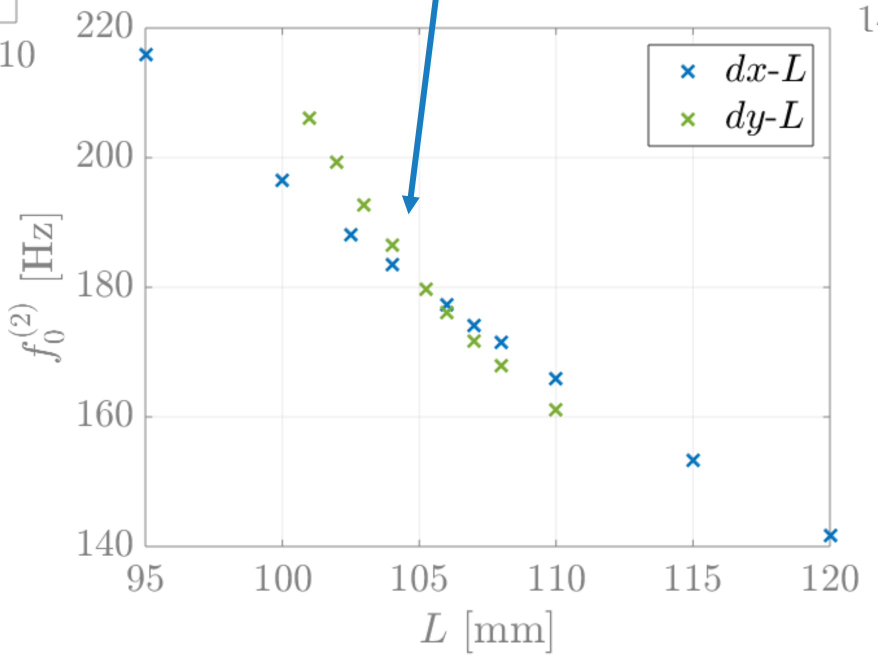

***dx* has the strongest impact on the restoring moment**

dx is used to guarantee the **equilibrium**

***L* has the strongest impact on $\boldsymbol{f_0^{(2)}}$**

Use a **shorter** blade to increase $\boldsymbol{f_0^{(2)}}$

Numerical validation - Locus

L fix, *dx* and *dy* vary

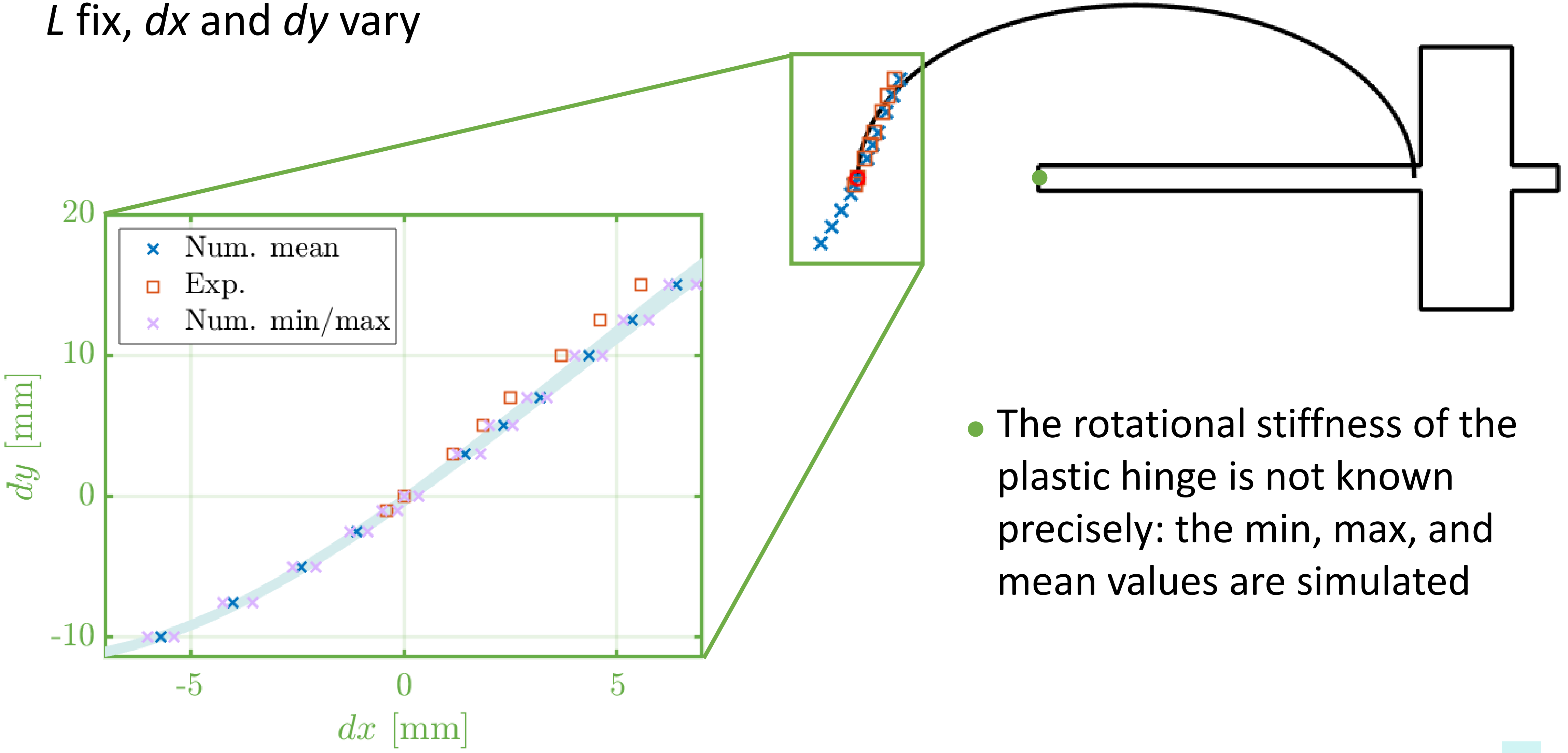

- The rotational stiffness of the plastic hinge is not known precisely: the min, max, and mean values are simulated

Numerical validation – Resonance frequency

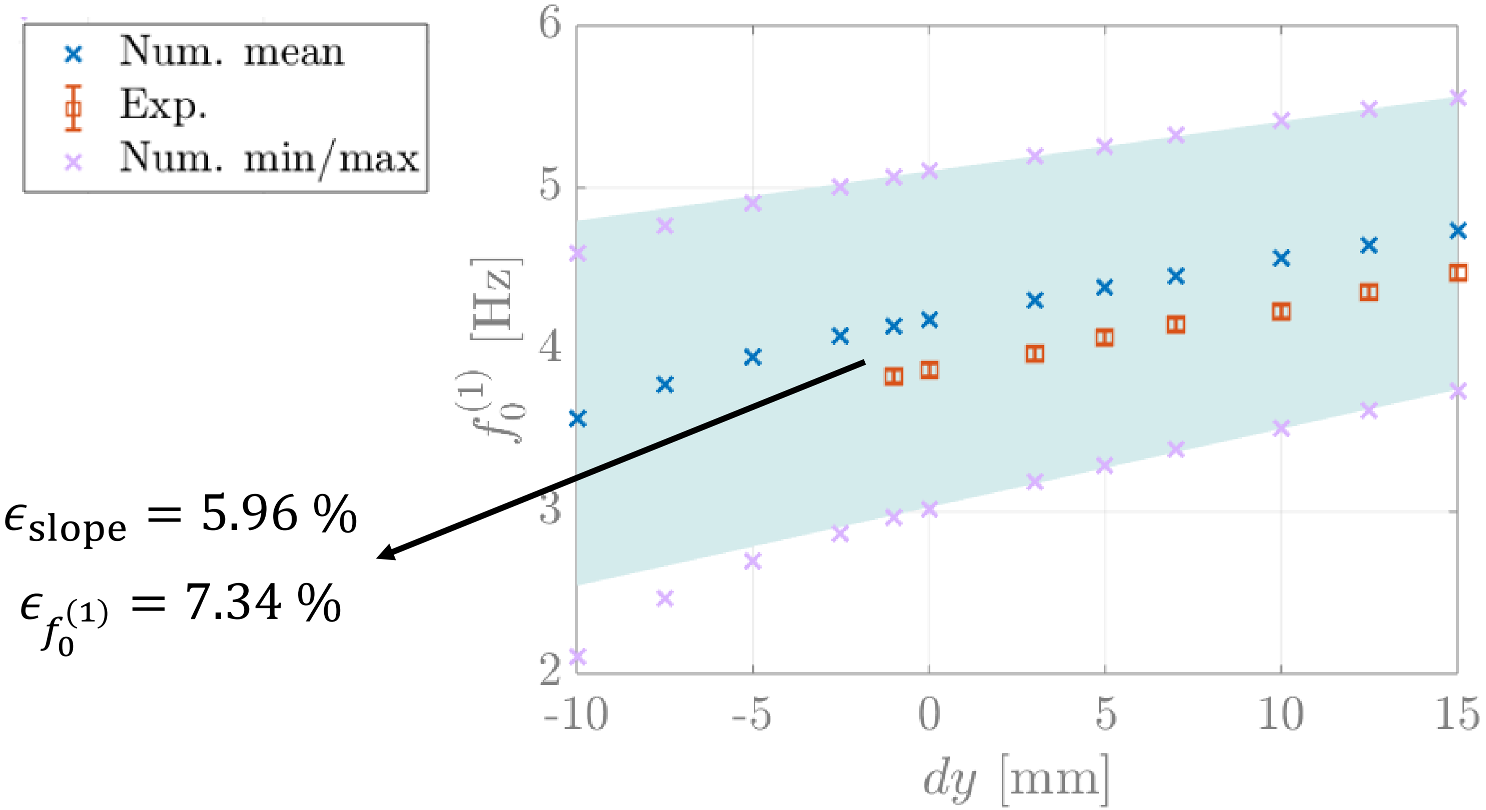

$\epsilon_{\text{slope}} = 5.96\ \%$

$\epsilon_{f_0^{(1)}} = 7.34\ \%$

Valid numerical model

Locus & curvature

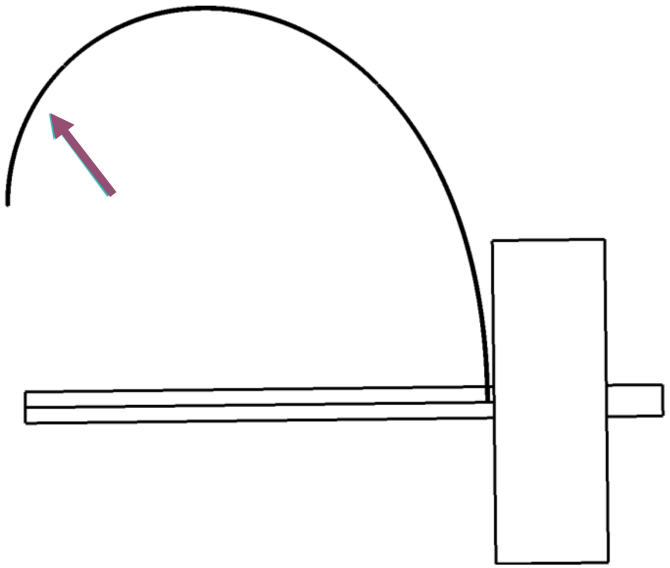

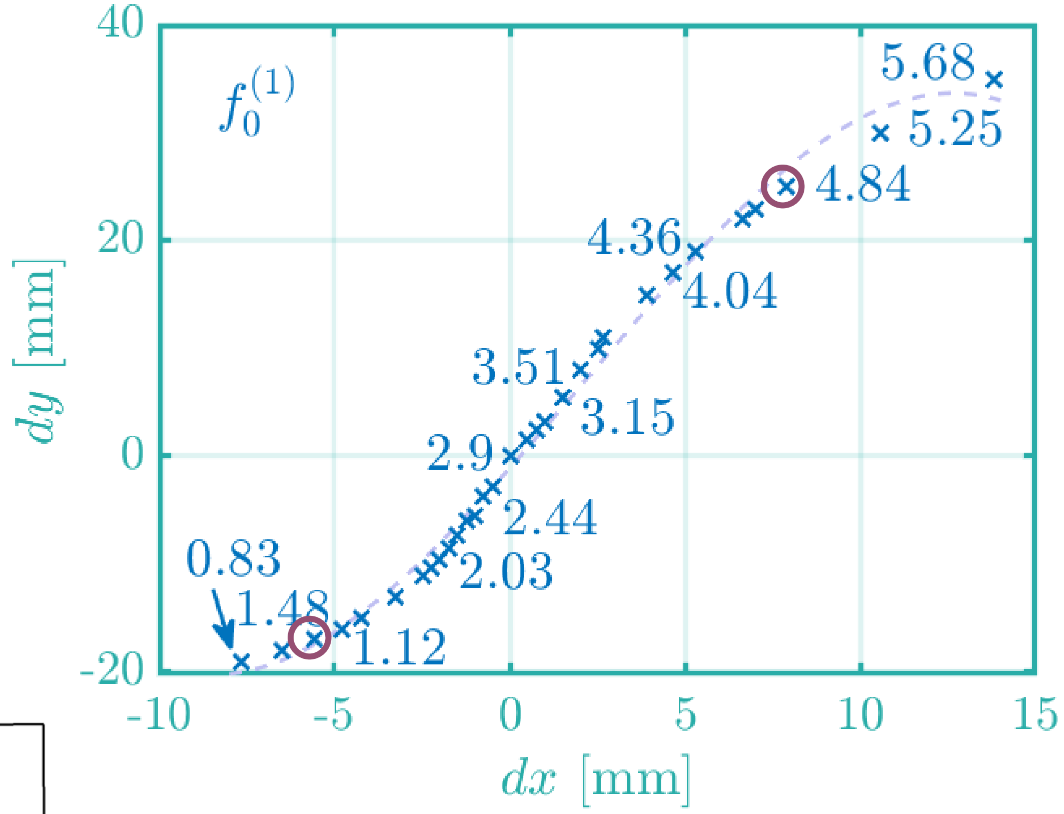

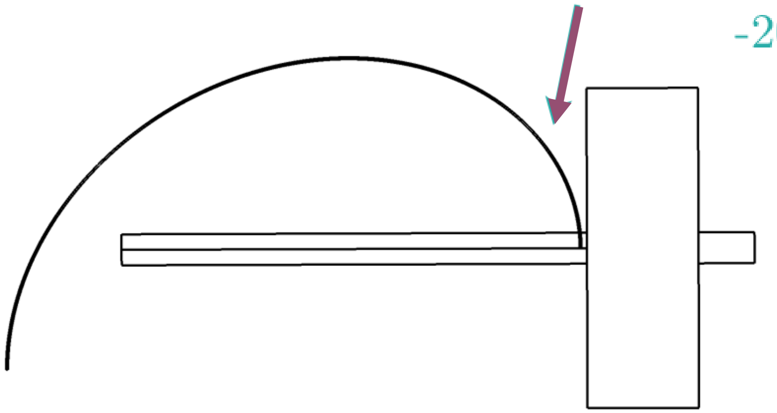

Influence of the hinge stiffness

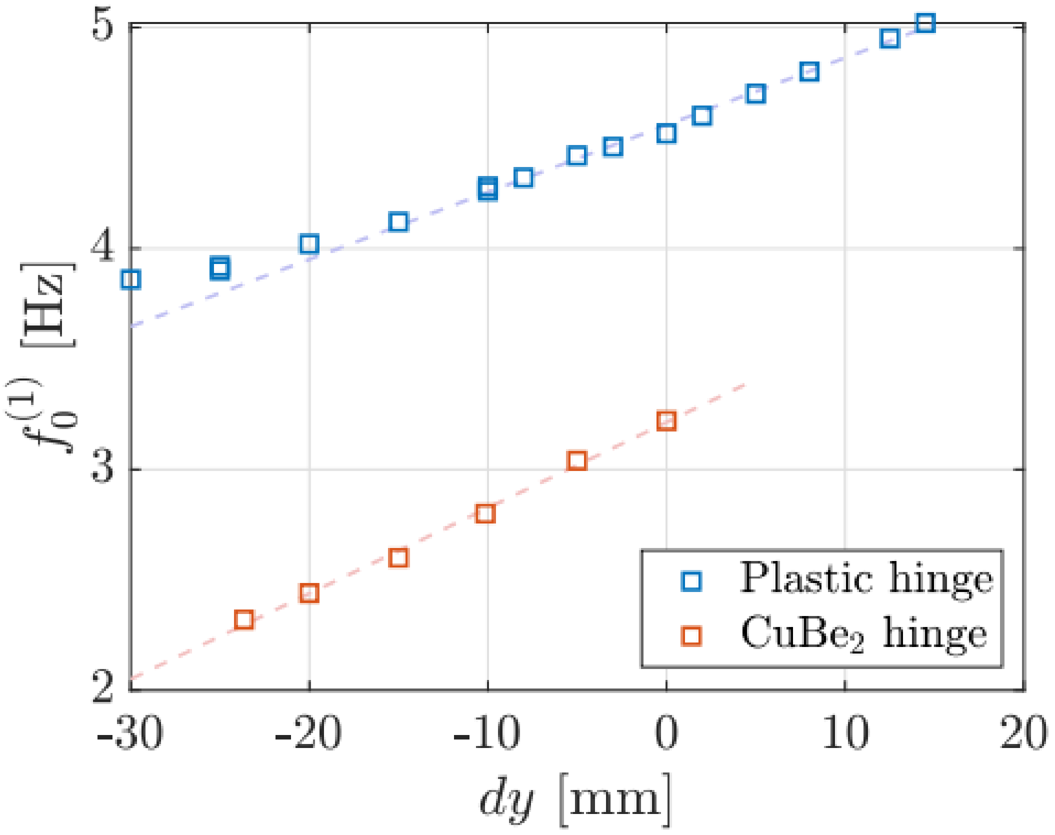

$$f_0^{(1)} = \frac{1}{2\pi}\sqrt{\frac{k_{\mathrm{LF}} + k_{\mathrm{flex}}}{I}}$$